Rise and Fall of the Beringian Steppe Bison
Beth Shapiro, *et al.*
Science **306**, 1561 (2004);
DOI: 10.1126/science.1101074

Science (print ISSN 0036-8075; online ISSN 1095-9203) is published weekly, except the last week in December, by the American Association for the Advancement of Science, 1200 New York Avenue NW, Washington, DC 20005.

3). Thus, deletion of JNK2 in macrophages was sufficient to decrease atherogenesis.

Two receptors appear to be essential in foam cell formation and receptor-mediated binding and uptake of modified lipoproteins: CD36 and scavenger receptor A (SR-A) (*20*). Immunofluorescence analyses revealed that expression of CD36 was unchanged in acLDL-stimulated peritoneal $ApoE^{-/-}$ $JNK2^{-/-}$ macrophages (Fig. 4A and fig. S7A). However, analyses with antibodies to SR-A showed increased abundance of this receptor (Fig. 4B and fig. S7B) ($P < 0.01$). Protein immunoblotting confirmed increased abundance of SR-A in protein extracts prepared from macrophages stimulated with acLDL. Amounts of SR-A were not altered in response to acLDL in double knockout or control animals (fig. S7C). $ApoE^{-/-}$ $JNK2^{-/-}$ macrophages formed filopodia-like projections, which were not observed in controls (Fig. 4C). This cellular phenotype is associated with increased adhesion and has been described in macrophages overexpressing SR-A (*21*). To examine whether increased abundance of SR-A in cultured macrophages also occurred in vivo, we used immunohistochemistry to detect SR-A on plaques from $ApoE^{-/-}$ $JNK2^{-/-}$ mice and $ApoE^{-/-}$ control mice. Increased amounts of SR-A were detected in macrophages in plaques of $ApoE^{-/-}$ $JNK2^{-/-}$ mice compared to those of control mice (Fig. 4D).

Alternative splicing results in three types of SR-A transcripts in humans. Occurrence of the Type III SR-A blocks modified LDL uptake (*22*). Therefore, we analyzed the expression of all three splicing variants in macrophages by semiquantitative RT-PCR using specific primers. We could not detect Type III mRNA in macrophages of either genotype. Type I and Type II mRNA was not increased in the absence of JNK2 (fig. S7D). Expression of CD36 or peroxisome proliferator–actived receptor (PPARγ) (*23*), was also not affected. Activation of the well-known JNK target c-jun in aortas from $ApoE^{-/-}$ and $ApoE^{-/-}$ $JNK2^{-/-}$ mice fed either a normal or high-cholesterol diet was not affected, suggesting that c-jun-dependent gene expression was not impaired (fig. S7E). Phosphorylation of SR-A on specific serines is essential for SR-A–dependent processing of modified LDL and for surface expression of SR-A (*24*–*26*). We immunoprecipitated SR-A from total protein extracts of $JNK2^{-/-}$ macrophages and corresponding wild-type cells. Western blotting of immunoprecipitated SR-A revealed an increased amount of SR-A in $JNK2^{-/-}$ cells compared to wild-type cells (Fig. 4, E and F). Blotting with phosphoserine-specific antibody indicated that the amount of serine-phosphorylated SR-A was lower in $JNK2^{-/-}$ extracts even though more SR-A protein was present (Fig. 4E). We confirmed decreased phosphorylation of SR-A after labeling of $JNK2^{-/-}$ macrophages with [^{32}P] orthophosphoric acid (Fig. 4F).

In this study, we provide in vivo evidence that JNK2 is required in a mouse model of atherogenesis. At the molecular level, we propose that JNK2-dependent decrease of SR-A phosphorylation and increase in SR-A abundance may lead to decreased internalization and degradation of receptor-bound modified LDL and as a consequence to reduced foam cell formation. Indeed, macrophage-specific overexpression of SR-A has been shown to be sufficient to reduce atherosclerosis in ApoE-deficient mice (*27*). In conclusion, specific inhibition of JNK2 activity may provide a therapeutic approach to decrease atheroma formation in patients.

References and Notes

1. P. Libby, *Nature* **420**, 868 (2002).
2. C. K. Glass, J. L. Witztum, *Cell* **104**, 503 (2001).
3. S. Gupta *et al.*, *EMBO J.* **15**, 2760 (1996).
4. C. Dong *et al.*, *Nature* **405**, 91 (2000).
5. J. Hirosumi *et al.*, *Nature* **420**, 333 (2002).
6. Z. Han, L. Chang, Y. Yamanishi, M. Karin, G. S. Firestein, *Arthritis Rheum.* **46**, 818 (2002).
7. A. M. Manning, R. J. Davis, *Nature Rev. Drug Discov.* **2**, 554 (2003).
8. A. S. Plump *et al.*, *Cell* **71**, 343 (1992).
9. Y. S. Heo *et al.*, *EMBO J.* **23**, 2185 (2004).
10. M. I. Cybulsky *et al.*, *J. Clin. Invest.* **107**, 1255 (2001).
11. Z. M. Dong, A. A. Brown, D. D. Wagner, *Circulation* **101**, 2290 (2000).
12. G. K. Hansson, P. Libby, U. Schonbeck, Z. Q. Yan, *Circ. Res.* **91**, 281 (2002).
13. D. D. Yang *et al.*, *Immunity* **9**, 575 (1998).
14. H. M. Dansky, S. A. Charlton, M. M. Harper, J. D. Smith, *Proc. Natl. Acad. Sci. U.S.A.* **94**, 4642 (1997).
15. A. Daugherty *et al.*, *J. Clin. Invest.* **100**, 1575 (1997).
16. C. Dong *et al.*, *Science* **282**, 2092 (1998).
17. V. J. Dzau, R. C. Braun-Dullaeus, D. G. Sedding, *Nature Med.* **8**, 1249 (2002).
18. Y. Zhan *et al.*, *Arterioscler. Thromb. Vasc. Biol.* **23**, 795 (2003).
19. A. C. Li, C. K. Glass, *Nature Med.* **8**, 1235 (2002).
20. V. V. Kunjathoor *et al.*, *J. Biol. Chem.* **277**, 49982 (2002).
21. S. R. Post *et al.*, *J. Lipid Res.* **43**, 1829 (2002).
22. P. J. Gough, D. R. Greaves, S. Gordon, *J. Lipid Res.* **39**, 531 (1998).
23. P. Tontonoz, L. Nagy, J. G. Alvarez, V. A. Thomazy, R. M. Evans, *Cell* **93**, 241 (1998).
24. H. Heider, E. S. Wintergerst, *FEBS Lett.* **505**, 185 (2001).
25. L. G. Fong, D. Le, *J. Biol. Chem.* **274**, 36808 (1999).
26. N. Kosswig, S. Rice, A. Daugherty, S. R. Post, *J. Biol. Chem.* **278**, 34219 (2003).
27. S. C. Whitman, D. L. Rateri, S. J. Szilvassy, J. A. Cornicelli, A. Daugherty, *J. Lipid Res.* **43**, 1201 (2002).
28. Macrophages were pulse-labeled with [^{32}P]orthophosphoric acid in sodium-phosphate-deficient culture medium 12 hours before harvesting.

29. We thank P. Lerch who provided us with oxLDL; D. Zhang and P. Meier, who helped us with isolation of aortas; H. Joch and A. Jaschko, who helped us with smooth muscle cell isolation; P. Bargsten, who helped us with bone marrow transplantation experiments; W. Krek and P. J. Gough, with whom we had very fruitful scientific discussions; and R. Eferl, for critical reading. Supported by the Swiss National Science Foundation (grant no. 3100-068118), the European Union (grant no. G5RD-CT-2001-00532), the Bundesamt für Bildung und Wissenschaft, and the Swiss Heart Foundation, and the "Forschungskredit 2003" of the University of Zurich.

Supporting Online Material

www.sciencemag.org/cgi/content/full/306/5701/1558/DC1
Materials and Methods
Figs. S1 to S7
References and Notes

23 June 2004; accepted 13 October 2004

Rise and Fall of the Beringian Steppe Bison

Beth Shapiro,[1,2] Alexei J. Drummond,[2] Andrew Rambaut,[2] Michael C. Wilson,[3] Paul E. Matheus,[4] Andrei V. Sher,[5] Oliver G. Pybus,[2] M. Thomas P. Gilbert,[1,2] Ian Barnes,[6] Jonas Binladen,[7] Eske Willerslev,[1,7] Anders J. Hansen,[7] Gennady F. Baryshnikov,[8] James A. Burns,[9] Sergei Davydov,[10] Jonathan C. Driver,[11] Duane G. Froese,[12] C. Richard Harington,[13] Grant Keddie,[14] Pavel Kosintsev,[15] Michael L. Kunz,[16] Larry D. Martin,[17] Robert O. Stephenson,[18] John Storer,[19] Richard Tedford,[20] Sergei Zimov,[10] Alan Cooper[1,2]*

The widespread extinctions of large mammals at the end of the Pleistocene epoch have often been attributed to the depredations of humans; here we present genetic evidence that questions this assumption. We used ancient DNA and Bayesian techniques to reconstruct a detailed genetic history of bison throughout the late Pleistocene and Holocene epochs. Our analyses depict a large diverse population living throughout Beringia until around 37,000 years before the present, when the population's genetic diversity began to decline dramatically. The timing of this decline correlates with environmental changes associated with the onset of the last glacial cycle, whereas archaeological evidence does not support the presence of large populations of humans in Eastern Beringia until more than 15,000 years later.

Climatic and environmental changes during the Pleistocene epoch [from 2 million years ago (Ma) to 10,000 years before the present (ky B.P.)] played an important role in the distribution and diversity of modern plants and animals (*1*, *2*). In Beringia, local climate

and geology created an ice-free refugium stretching from eastern Siberia to Canada's Northwest Territories (*3*). Periodic exposure of the Bering Land Bridge facilitated the exchange of a diverse megafauna (such as bison, mammoth, and musk ox) supported by tundra-steppe grasses and shrubs (*3*, *4*). Humans are believed to have colonized North America via this route, and the first well-accepted evidence of human settlement in Alaska dates to around 12 ky B.P. (*5*). The latest Pleistocene saw the extinction of most Beringian megafauna including mammoths, short-faced bears, and North American lions. The reasons for these extinctions remain unclear but are attributed most often to human impact (*6*, *7*) and climate change associated with the last glacial cycle (*8*).

Pleistocene bison fossils are abundant across Beringia and they provide an ideal marker of environmental change. Bison are believed to have first entered eastern Beringia from Asia during the middle Pleistocene [marine oxygen isotope stages (MISs) 8 to 6, circa (ca.) 300 to 130 ky B.P.] and then moved southward into central North America during the MIS 5 interglacial period (130 to 75 ky B.P.), where they were distributed across the continental United States (*9*). During this time, Beringian and central North American bison populations may have been periodically separated by glacial ice that formed over most of Canada (*10*, *11*). The timing and extent of genetic exchange between these areas remain unclear (*2*).

The abundance and diversity of bison fossils have prompted considerable paleontological and archaeological research into their use as stratigraphic markers. Extensive morphological diversity, however, has complicated discrimination between even the most accepted forms of fossil bison, and the lack of stratigraphy in Beringian sites has prevented the development of a chronological context. These complications create a complex literature of conflicting hypotheses about bison taxonomy and evolution (*9*, *12*). After a severe population bottleneck, which ocurred only 200 years ago (*13*), two subspecies survive in North America: *Bison bison bison*, the plains bison, and *B. b. athabascae*, the wood bison (*9*, *13*).

To investigate the evolution and demographic history of Pleistocene bison, we collected 442 bison fossils from Alaska, Canada, Siberia, China, and the lower 48 United States (*14*). We used ancient DNA techniques to sequence a 685–base pair (bp) fragment of the mitochondrial control region (*14*). Accelerator mass spectrometry radiocarbon dates were obtained for 220 samples, which spanned a period of >60 ky (*14*).

The association of radiocarbon dates with DNA sequences enables the calibration of evolutionary rates within individual species (*15*). Bayesian phylogenetic analyses produced an evolutionary rate estimate for the bison mitochondrial control region of 32% per million years (My) [95% highest posterior density (HPD): 23 to 41% per My] (*14*). This estimate is independent of paleontological calibrations but agrees with fossil-calibrated rates for cattle of 30.1% per My (*16*) and 38% per My (*17*). This rate was used to calculate the ages of key nodes in the bison genealogy (*14*). The most recent common ancestor (MRCA) of all bison included in this analysis lived around 136 ky B.P. (95% HPD: 164 to 111 ky B.P.). In the majority (66%) of estimated trees, Eurasian bison cluster into a single clade, with a MRCA between 141 and 89 ky B.P. Although

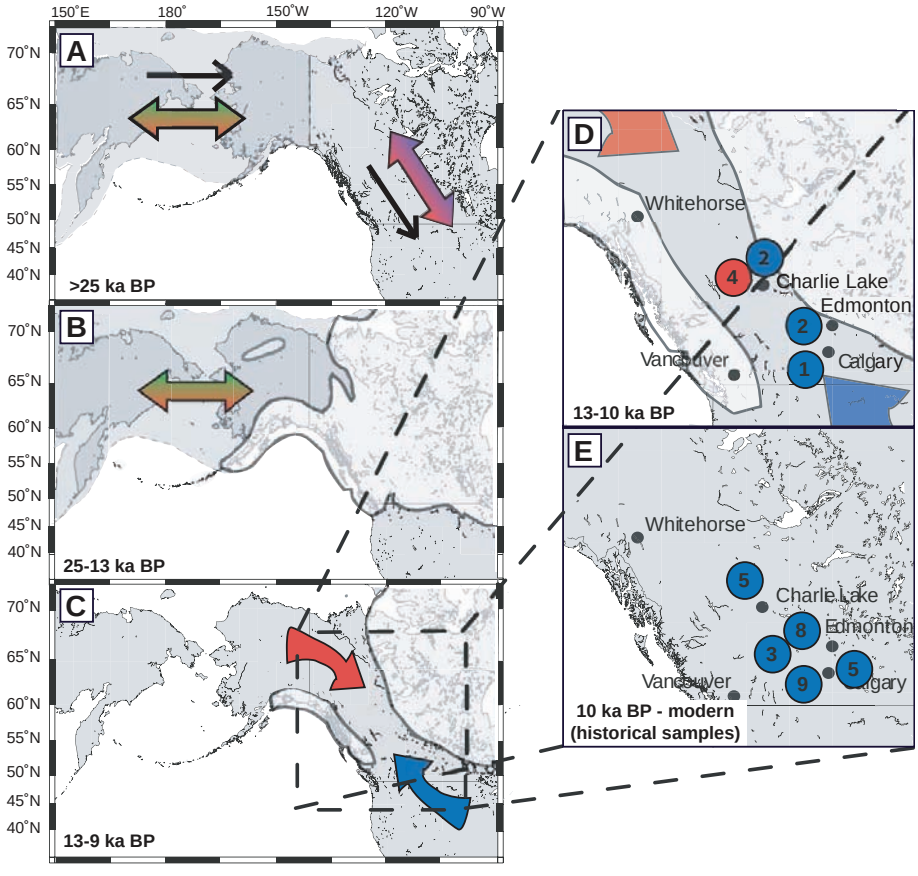

Fig. 1. Distribution of bison in Beringia and central North America through time. (**A** to **C**) Double-headed arrows show gene flow between regions. Black arrows indicate colonization events. Circles in maps (**D**) and (**E**) designate either northern (red) or southern (blue) ancestry and the number of samples from that location.

[1]Henry Wellcome Ancient Biomolecules Centre, [2]Department of Zoology, Oxford University, South Parks Road, Oxford OX13PS, UK. [3]Department of Geology and Department of Anthropology, Douglas College, Post Office Box 2503, New Westminster, British Columbia V3L 5B2, Canada. [4]Alaska Quaternary Center and Institute of Arctic Biology, University of Alaska Fairbanks, 900 Yukon Drive, Fairbanks, AK 99775–5940, USA. [5]Severtsov Institute of Ecology and Evolution, Russian Academy of Sciences, 33 Leninsky Prospect, 119071 Moscow, Russia. [6]The Centre for Genetic Anthropology, Department of Biology, Darwin Building, University College London, Gower Street, London WC1E 6BT, UK. [7]Department of Evolutionary Biology, Zoological Institute, University of Copenhagen, Universitetsparken 15–2100 Copenhagen, Denmark. [8]Zoological Institute, Russian Academy of Sciences, 199034 St. Petersburg, Russia. [9]Quaternary Paleontology, Provincial Museum of Alberta, Edmonton, Alberta T5N 0M6, Canada. [10]North-East Scientific Station of Russian Academy of Science, Post Office Box 18, Cherskii, Republic Sakha-Yakutia, Russia. [11]Department of Archaeology, Simon Fraser University, Burnaby, British Columbia V5A 1S6, Canada. [12]Department of Earth and Atmospheric Sciences, University of Alberta, Edmonton, Alberta T6G 2E3, Canada. [13]Canadian Museum of Nature (Paleobiology), Ottawa, Ontario K1P 6P4, Canada. [14]Department of Archaeology, Royal British Columbia Museum, 675 Belleville Street, Victoria, British Columbia V8V 1X4, Canada. [15]Institute of Plant and Animal Ecology, Russian Academy of Sciences, 202 8 Martas Street, Ekaterinburg 620144, Russia. [16]Bureau of Land Management, 1150 University Avenue, Fairbanks, AK 99708 USA. [17]Department of Ecology and Evolutionary Biology, University of Kansas, Lawrence, KS 66045, USA. [18]Alaska Department of Fish and Game, 1300 College Road, Fairbanks, AK 99701, USA. [19]Yukon Paleontologist, Heritage Resources, Yukon Department of Tourism and Culture, Box 2703, Whitehorse, Yukon Territory YTY1A 2C6, Canada. [20]Department of Paleontology, American Museum of Natural History, Central Park West at 79th Street, New York, NY 10024, USA.

*To whom correspondence should be addressed. E-mail: alan.cooper@zoo.ox.ac.uk

these two estimates overlap, the age of the MRCA of Eurasian bison was the same as that of the root in 4.8% of 135,000 posterior genealogies (with a Bayes factor of 20.83 that the Eurasian MRCA is not also the MRCA of all clades), suggesting that the Eurasian clade is not the oldest in the tree. This suggests that late Pleistocene bison from the Ural Mountains to northern China are descendants of one or more dispersals from North America. Several North American lineages fall within the Eurasian clade, indicating subsequent asymmetric genetic exchange, predominantly from Asia to North America.

Figure 1A depicts inferred gene flow between bison populations in Beringia and central North America during MIS 3 (~60 to 25 ky B.P.), which is the interstadial period before the Last Glacial Maximum (LGM, ca. 22 to 18 ky B.P.). Bison were continuously distributed from eastern Beringia southward into central North America during this period, before the formation of the Laurentide (eastern) and Cordilleran (western) ice sheets created a barrier to north-south faunal exchange. Although any coalescence between these ice masses was brief (*11*), the absence of faunal remains aged 22 to12 ky B.P. (Fig. 1B) (*18*) indicates that the area was uninhabitable by large mammals during this time. Bison fossils in central North America during the LGM are sparsely distributed across the continent (*9*). DNA could be retrieved only from two specimens from this period, both from Natural Trap Cave, Wyoming (20,020 ± 150 and 20,380 ± 90 ky B.P.). These specimens are not closely related (*14*), indicating that populations south of the ice retained some genetic diversity until the LGM.

The ice sheets began to retreat around 14 ky B.P., forming an ice-free corridor (IFC) through which dispersal between Beringia and North America could occur. The first observed bison haplotypes in the IFC are southern in origin (Fig. 1, C and D), with the oldest specimen being in southern Alberta by 11.3 ky B.P., and others near Athabasca, northern Alberta, by 10.4 ky B.P. This finding is consistent with evidence that the first faunal assemblages and archaeological presence in the IFC were southern in origin (*18–20*). The opening of the northern end of the IFC saw a limited southward dispersal of Beringian bison, with a subset of the northern diversity found near the Peace River (northwestern British Columbia) by 11.2 to 10.2 ky B.P. (Fig. 1C) (*14*). Southern bison are also found in this area around 10.5 ky B.P., making it the only location where post-LGM northern and southern clades occurred at the same time. Subsequent genetic exchange between Beringia and central North America was limited by the rapid establishment of spruce forest across Alberta around 10 ky B.P. (*21*) and by the widespread development of peatland across western and northwestern Canada (*22*). North of these ecological barriers, grasslands were reduced by invading trees and shrubs, yet despite the decrease in quality and quantity of habitat (*3*), bison persisted in eastern Beringia until a few hundred years ago (*14*, *23*).

It has been hypothesized that modern bison descended from Beringian bison that moved south through the IFC after the LGM (*9*, *19*) and have since undergone a decline in diversity due to over-hunting and habitat loss (*13*). In contrast, our data show that modern bison are descended from populations that were south of the ice before the LGM and that diversity has been restricted to at least 12 ky B.P., around the time of the megafaunal extinctions. All modern bison belong to a clade distinct from Beringian bison. This clade has a MRCA between 22 and 15 ky B.P., which is coincident with the separation of northern and southern populations by the western Canadian ice barrier. This clade diverged from Beringian bison by 83 to 64 ky B.P. and was presumably part of an early dispersal from Beringia, as indicated by the long branch separating it from Beringian bison (*14*). If other remnants of these early dispersals survived the LGM, they contributed no mitochondrial haplotypes to modern populations.

Coalescent theory is used to evaluate the likelihood of a demographic history, given plausible genealogies (*24*). Under a coalescent model, the timing of divergence dates provides information about effective population sizes through time. To visualize this for bison, a technique called the skyline plot was used (*14*, *25*). The results showed two distinct demographic trends since the MRCA, suggesting that a simple demographic model, such as constant population size or exponential growth, was insufficient to explain the evolutionary history of Beringian bison. We therefore extended the Bayesian coalescent method (*26*) to a two-epoch demographic model with exponential population growth at rate r_{early}, until a transition time, t_{trans}, after which a new exponential rate, r_{late}, applies until the present effective population size, N_0, is reached (Fig. 2A). In this model, both the early and late epochs can have positive or negative growth rates, with both the rates and the time of transition estimated directly from the data.

The analysis strongly supported a boom-bust demographic model (Table 1), in which

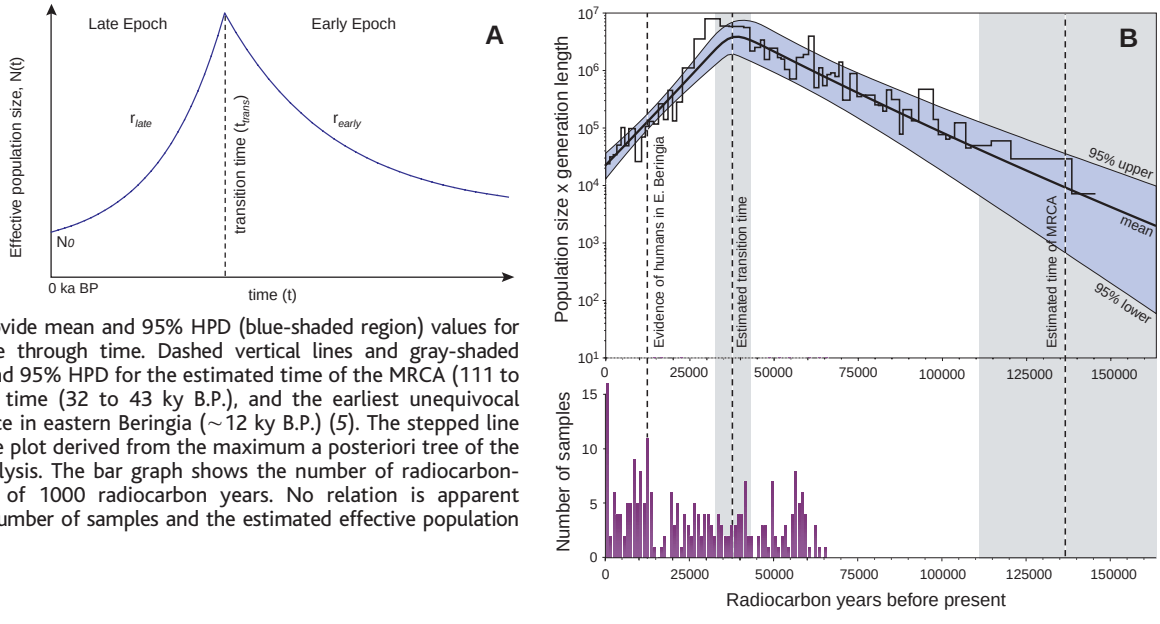

Fig. 2. (**A**) The two-epoch demographic model with four demographic parameters: N_0, r_{early}, r_{late}, and t_{trans}. The effective population size is a compound variable considered linearly proportional to census population size. (**B**) Log-linear plot describing the results of the full Bayesian analyses. Smoothed curves provide mean and 95% HPD (blue-shaded region) values for effective population size through time. Dashed vertical lines and gray-shaded regions describe mean and 95% HPD for the estimated time of the MRCA (111 to 164 ky B.P.), transition time (32 to 43 ky B.P.), and the earliest unequivocal reported human presence in eastern Beringia (~12 ky B.P.) (*5*). The stepped line is the generalized skyline plot derived from the maximum a posteriori tree of the exponential growth analysis. The bar graph shows the number of radiocarbon-dated samples in bins of 1000 radiocarbon years. No relation is apparent between the absolute number of samples and the estimated effective population size or transition time.

Table 1. Results of Bayesian analyses assuming constant population size, exponential growth, and a two-epoch model for the full analysis of 191 bison associated with finite radiocarbon dates (*14*). Model parameters are as defined in (*26*). The large difference between the mean goodness-of-fit statistics [ln(posterior)] indicates that under either the Akaike information criterion or Bayesian information criterion tests, the two-epoch model is a significantly better fit to the data than the simpler models.

	Constant size			Exponential growth			Two epoch		
	Lower	Mean	Upper	Lower	Mean	Upper	Lower	Mean	Upper
Age estimates (yr B.P.)									
Root height	117,000	152,000	189,000	113,000	146,000	181,000	111,000	136,000	164,000
Modern/southern clade	20,200	28,000	36,600	18,600	26,400	35,000	15,400	23,200	32,200
Eurasian clade	85,000	116,000	151,000	83,000	112,000	144,000	89,000	114,000	141,000
Model parameters									
Mean ln(posterior)		−6530.795			−6517.35			−6394.568	
Mutation rate (substitutions/site/year)	2.79×10^{-7}	3.78×10^{-7}	4.85×10^{-7}	2.30×10^{-7}	3.20×10^{-7}	4.13×10^{-7}	2.30×10^{-7}	3.20×10^{-7}	4.13×10^{-7}
Kappa	19	27	37	19	27.4	37	19	27	37
Shape parameter	0.22	0.35	0.49	0.22	0.35	0.49	0.22	0.35	0.5
Proportion of invariant sites	0.33	0.45	0.56	0.33	0.45	0.56	0.34	0.45	0.56

an exponential expansion of the bison population was followed by a rapid decline, with a transition around 37 ky B.P. (Fig. 2B). At the height of the boom, the population size was around 230 times (95% HPD: 71 to 454 times) that of the modern population. When this model is applied to the modern clade alone, a growth period peaks around 1000 years ago (95% HPD: 63 to 2300 yr B.P.) and is followed by a rapid decline (*14*), which is consistent with historical records of a population bottleneck in the late 1800s (*13*). These results illustrate the power of this method to recover past demographic signals.

The effects of population subdivision and patch extinction and recolonization on coalescence patterns have not been fully characterized, yet they can influence demographic estimates such as skyline plots (*27*). To test for the effect of population subdivision on our models, the two-epoch analysis was repeated first without the Eurasian bison and then without both Eurasian and central North American bison. The results of these analyses were consistent with those for the entire data set (*14*), suggesting that the assumption of panmixia does not affect the analysis. These results suggest that the major signal for the boom-bust scenario came from the well-represented eastern Beringian population.

The timing of the decline in Beringian bison populations (Fig. 2B) predates the climatic events of the LGM and events at the Pleistocene-Holocene boundary. The bison population was growing rapidly throughout MIS 4 and 3 (~75 to 25 ky B.P.), approximately doubling every 10,200 (95% HPD: 7500 to 15,500) years. The reversal of this doubling trend at 42 to 32 ky B.P. and the subsequent dramatic decrease in population size are coincident with the warmest part of MIS 3, which is marked by a reduction in steppe-tundra due to treecover reaching its late Pleistocene maximum (*28*). Modern boreal forests serve as a barrier to bison dispersal because they are difficult to traverse and provide few food sources (*3*). After the interstadial, cold and arid conditions increasingly dominated, and some component of these ecological changes may have been sufficient to stress bison populations across Beringia. Previous reports of local extinction of brown bears (*29*) and hemionid horses (*8*) in Alaska around 32 to 35 ky B.P. support the possibility of a larger scale environmental change affecting populations of large mammals.

These results have considerable implications for understanding the end-Pleistocene mass extinctions, because they offer the first evidence of the initial decline of a population, rather than simply the resulting extinction event. These events predate archaeological evidence of significant human presence in eastern Beringia (*5*), arguing that environmental changes leading up to the LGM were the major cause of the observed changes in genetic diversity. If other species were similarly affected, differences in how these species responded to environmental stress may help to explain the staggered nature of the megafaunal extinctions (*7*, *30*). However, it is possible that human populations were present in eastern Beringia by 30 ky B.P., with reports of human-modified artifacts as old as 42 to 25 ky B.P. from the Old Crow basin in Canada's Yukon Territory (*31*). Although the archaeological significance of these specimens is disputed and the number of individuals would be low, the specimens are consistent with the timing of the population crash in bison. This emphasizes that future studies of the end–Pleistocene mass extinctions in North America should include events before the LGM.

Ancient DNA is a powerful tool for studying evolutionary processes such as the response of organisms to environmental change. It should be possible to construct a detailed paleoecological history for late Pleistocene Beringia using similar methods for other taxa. Almost none of the genetic diversity present in Pleistocene bison survived into Holocene populations, erasing signals of the complex population dynamics that took place as recently as 10,000 years ago.

References and Notes

1. G. Hewitt, *Nature* **405**, 907 (2000).
2. R. W. Graham *et al.*, *Science* **272**, 1601 (1996).
3. R. D. Guthrie, *Frozen Fauna of the Mammoth Steppe* (Univ. of Chicago Press, Chicago, 1990).
4. G. D. Zazula *et al.*, *Nature* **423**, 603 (2003).
5. D. R. Yesner, *Quat. Sci. Rev.* **20**, 315 (2001).
6. B. W. Brook, D. Bowman, *J. Biogeogr.* **31**, 517 (2004).
7. J. Alroy, *Science* **292**, 1893 (2001).
8. R. D. Guthrie, *Nature* **426**, 169 (2003).
9. J. N. McDonald, *North American Bison: Their Classification and Evolution* (Univ. of California Press, Berkeley, CA, 1981).
10. C. A. S. Mandryk, H. Josenhans, D. W. Fedje, R. W. Matthewes, *Quat. Sci. Rev.* **20**, 301 (2001).
11. A. S. Dyke *et al.*, *Quat. Sci. Rev.* **21**, 9 (2002).
12. M. F. Skinner, O. C. Kaisen, *Bull. Am. Mus. Nat. Hist.* **89**, 126 (1947).
13. F. G. Roe, *The North American Buffalo,* (Univ. of Toronto Press, Toronto, ON, ed. 2, 1970).
14. Materials and methods are available as supporting material on *Science* Online.
15. D. M. Lambert *et al.*, *Science* **295**, 2270 (2002).
16. D. G. Bradley, D. E. MacHugh, P. Cunningham, R. T. Loftus, *Proc. Natl. Acad. Sci. U.S.A.* **93**, 5131 (1996).
17. C. S. Troy *et al.*, *Nature* **410**, 1088 (2001).
18. J. A. Burns, *Quat. Int.* **32**, 107 (1996).
19. M. C. Wilson, *Quat. Int.* **32**, 97 (1996).
20. J. C. Driver, in *People and Wildlife in Northern North America*, S. C. Gerlach, M. S. Murray, Eds. (British Archaeological Reports, International Series 944, Archaeopress, Oxford, 2001), pp. 13–22.
21. N. Catto, D. G. E. Liverman, P. T. Bobrowsky, N. Rutter, *Quat. Int.* **32**, 21 (1996).
22. L. A. Halsey, D. H. Vitt, I. E. Bauer, *Clim. Change* **40**, 315 (1998).
23. R. O. Stephenson *et al.*, in *People and Wildlife in Northern North America*, S. C. Gerlach, M. S. Murray, Eds. (British Archaeological Reports, International Series 944, Archaeopress, Oxford, 2001), pp. 125–148.
24. R. C. Griffiths, S. Tavare, *Philos. Trans. R. Soc. London Ser. B* **344**, 403 (1994).

25. K. Strimmer, O. G. Pybus, *Mol. Biol. Evol.* **18**, 2298 (2001).
26. A. J. Drummond, G. K. Nicholls, A. G. Rodrigo, W. Solomon, *Genetics* **161**, 1307 (2002).
27. J. R. Pannell, *Evolution* **57**, 949 (2003).
28. P. M. Anderson, A. V. Lozhkin, *Quat. Sci. Rev.* **20**, 93 (2001).
29. I. Barnes, P. E. Matheus, B. Shapiro, D. Jensen, A. Cooper, *Science* **295**, 2267 (2002).
30. D. K. Grayson, D. J. Meltzer, *J. Archaeol. Sci.* **30**, 585 (2003).
31. R. E. Morlan, *Quat. Res.* **60**, 123 (2003).
32. We thank the museums and collections that donated material and T. Higham, A. Beaudoin, K. Shepherd, R. D. Guthrie, B. Potter, C. Adkins, D. Gilichinsky, R. Gangloff, S. C. Gerlach, C. Li, N. K. Vereshchagin, T. Kuznetsova, G. Boeskorov, the Alaska Bureau of Land Management, and the Yukon Heritage Branch for samples, logistical support, and assistance with analyses. We thank D. Rubenstein, R. Fortey, and P. Harvey for comments on the manuscript; Balliol College; the Royal Society; the Natural Environment Research Council; the Biotechnology and Biological Sciences Research Council; Rhodes Trust; Wellcome and Leverhulme Trusts for financial support; and Oxford Radiocarbon Dating Service and Lawrence Livermore National Laboratory for carbon dating.

Supporting Online Material
www.sciencemag.org/cgi/content/full/306/5701/1561/DC1
Materials and Methods
SOM Text
Figs. S1 to S5
Tables S1 to S4
References

4 June 2004; accepted 4 October 2004

Rise and fall of the Beringian Steppe bison

Supporting Online Material:

Materials and Methods

(a.) DNA extraction and amplification:

DNA was extracted from 442 fossil bison ranging in age from modern to >60 ka BP (Figure S1, Table S1). Samples included individuals from Eastern Beringia, Western Beringia, China, the Russian Urals and North America south of the ice. The European bison, *Bison bonasus*, is genetically distant from the North American bison(*S1*,*S2*), and was not considered in these analyses.

Stringent aDNA protocols are especially necessary for population studies(*S3*), and all DNA extractions and PCR reactions were set-up and performed accordingly in a geographically isolated, specialist aDNA laboratory at the Oxford University Museum of Natural History. All subsequent molecular work, such as thermocycling, cloning, and sequencing, was performed in the DNA facility at the Department of Zoology. Total cellular DNA (nuclear and mitochondrial) was extracted according to the following protocol: First, the exterior surface of the sample was removed, and a 0.5-1g section was excised and powdered using an 8mm tungsten ball bearing in a Braun Mikrodismembrator U (B. Braun Biotech International, Germany) at 2000 rpm in sterilised stainless steel containers. The powder was decalcified overnight in 10-30 mL of 0.5M EDTA (pH8) at room temperature. The sediment was then collected by centrifugation and digested in 6-8 mL of extraction buffer containing 10mM Tris-HCL (pH 8.0), 10mM NaCl, 0.5 mg/ml proteinase K, 10 mg/mL dithiothreitol (DTT), 1% sodium dodecyl sulfate (SDS) and 0.001-0.01M N-phenacylthiazolium bromide (PTB). The extraction was incubated overnight at 50-55˚C. Following digestion, the extraction was added to an equal volume of Tris-saturated phenol and rotated constantly for 10 min. before centrifugation at 6000 rpm for an additional 10 min. The aqueous phase was then removed. This step was repeated twice, once with an equal volume of phenol and then with an equal volume of chloroform. The aqueous phase was purified and desalted with sequential additions to Centricon-30 microconcentrators (Amicon) and concentrated to approximately 75-100µL. DNA extractions were performed in batches of 6-28 samples, with at least one negative extraction control (no bone powder) used for every 14 samples run.

PCR amplifications were performed in 25µL reactions with 1µL of extract, 1.25 U Platinum *Taq* Hi-Fidelity and 1X buffer (Invitrogen Ltd., UK), 2mg/ml rabbit serum albumin (RSA; Sigma, fraction V), 2mM MgSO4, 250µM of each dNTP, and 1µM of each primer. PCR thermal cycling reactions were typically 94˚C for 2 min, followed by 35-40 cycles of 94˚C denaturation for 25-30 sec, annealing for 45 sec at various temperatures depending on the primers (details are available from

the authors on request), and extension at 68˚C for 45 sec. Amplicons were purified using the QiaGen PCR Purification Kit (QiaGen Ltd., UK) according to manufacturers instructions.

Negative extraction controls as well as negative PCR controls (no extract) were used in each reaction. In no instance was modern DNA used as a positive control. DNA was amplified using overlapping fragments ranging in length from 120-710 base-pairs (bp), depending on the condition of the specimen. Primers were designed to target an approximately 685-bp fragment. Primer sequences are listed in Table S2. Sequencing reactions were performed on both strands using a PRISM BigDye Terminator v2.0 or v3.x Cycle Sequencing Ready Reaction Kit (Applied Biosystems, UK). Reactions were performed in 10μL according to manufacturer's instructions. Unincorporated dye terminators and primers were removed by ethanol precipitation, and the pellet was then frozen and transferred to the DNA sequencing facility (Zoology department, Oxford University) where it was sequenced on an ABI 377, 310, or 3700 according to manufacturer's instructions.

Mitochondrial control region DNA was successfully amplified and sequenced from 352 of 442 specimens (79.6%), including specimens morphologically identified as *B. priscus, B. preoccidentalis, B. occidentalis*, and *B. antiquus.* Three wood bison predating the 1925 introduction of plains bison into Wood Buffalo National Park, Alberta and the Northwest Territories, were also included in the analysis. For 24 specimens, less than 2/3 of the total 685-bp target sequence could be amplified, and these were excluded from the phylogenetic analyses. The remaining 328 sequences were submitted to GenBank, with reference numbers AY748469-AY748796.

More than 200 individual products were cloned to evaluate template damage, detect co-amplification of numts, and to cross-check accuracy and contamination (Table S1). Cloning was performed using the Invitrogen (UK Ltd) Topo-TA cloning kit according to manufacturers instructions. In each experiment, 8-12 clones were sequenced as described above. No evidence of nuclear copies was detected, and over-lapping sequences consistently matched. Template damage was minimal, especially in permafrost-preserved specimens, which is consistent with theirgenerally excellent biochemical preservation. To check the accuracy of the extraction, amplification, and sequencing steps, sequences from 52 specimens were replicated (Table S1). Of these, 29 were replicated within the ABC using extractions chronologically separated by more than six months, 16 specimens were replicated at an aDNA facility in Copenhagen, Denmark (of which all steps were replicated for 10, and the amplification/sequencing steps were replicated for 6), and the remaining 8 were replicated at an aDNA facility at University College, London. Most replications were cloned, and in each instance produced consistent DNA sequences. The recovery of identical sequences from individual specimens despite the extensive diversity of detected bison mitochondrial sequences (Figs. S2-S4) provides additional support for the authenticity of the results. To avoid the risk of introducing possible contaminants, no modern bison DNA sequences were generated for the purpose of this

study. Instead, 22 modern bison sequences were obtained from GenBank (accession numbers AF083357-AF083364, U12935-6, U12941, U12943-U12948, U12955-U12959) and included in our analyses.

(b.) Phylogenetic and Demographic analyses:

Bayesian coalescent analysis using Markov Chain Monte Carlo (MCMC) was performed with the program BEAST(*S4, S5*). BEAST employs MCMC(*S6*) integration to produce a set of plausible trees, substitution rates, and demographic histories (the posterior) describing the ancestral history of the sampled sequences. The posterior represents the combined influence of prior knowledge (the coalescent model of evolution) and the likelihood of the observations (the DNA sequences and the radiocarbon dates) under the specified evolutionary model. To reduce the number of unknown parameters, the full-dataset Bayesian analyses were restricted to 169 sequences associated with finite radiocarbon ages (including two samples from Montana – BS 129 and BS368 – that are known to be historical samples < 200 years old) plus 22 previously published sequences from modern bison (GenBank Accession numbers AF083357-AF083364, U12935-6, U12941, U12943-U12948, U12955-U12959). Several demographic models were evaluated, and standard statistical methods were used to choose the best-fitting model(*S7*). A modified version of BEAST that included novel parametric demographic models (such as the two-epoch model described in the main text) was used to estimate the demographic history and genetic relationships among bison in Beringia and in central North America over the last 150 ka BP. Various demographic models of population growth and decline were assessed.

In each analysis, un-calibrated radiocarbon dates associated with specific DNA sequences were incorporated as prior information, using the carbon-14 half-life of 5568 years. Model parameters (gamma shape, proportion of invariant sites, transition/transversion ratio, and mutation rate) were co-estimated with population demographic parameters and genealogical divergence times. Five independent Markov chains were run for 30 million iterations each, starting from an independent random tree. To allow for convergence, the first 3 million iterations were discarded from each chain, and trees were sampled every 5000 iterations thereafter. Posterior probabilities were calculated for each divergence time from the combined set of 27,000 trees. The results are presented as the mean and 95% highest posterior density (HPD) limits. For an additional estimate of support, bootstrap re-sampling was performed using PAUP(*S8*), with 200 sample trees generated by NJ under a HKY+G+I model of evolution, with model parameters fixed to the mean values obtained from the Bayesian analysis.

Figure S2 shows (a) the Maximum *a posteriori* (MAP) tree of 135 million posterior trees resulting from the two-epoch Bayesian analysis of 169 ancient and 22 modern bison and (b) a NJ tree

detailing relationships among 352 specimens for which ≥2/3 of the 685-bp fragment was sequenced. The nodes separating the modern clade (clade 1a) from all other Beringian bison, and the small clade of Beringian bison that moved south into the ice-free corridor (IFC) following deglaciation (clade 4b), are highlighted. More detailed trees listing the provenance and radiocarbon dates from each of the samples are given in Figs. S3 and S4. Several specimens were morphologically identified as belonging to different *Bison* taxa (Table 1). Samples that were ascribed to particular taxa based on morphological grounds did not group together in the trees.

Changes in the size of the bison populations through time were additionally evaluated using the program GENIE(*S9*) to generate a generalised skyline plot. This highly parametric model uses the distribution of coalescence events in a single tree to estimate values for effective population size through time(*S10*). In contrast to the methods used in BEAST, which perform demographic inference on a set of possible trees, the skyline plot uses a single tree as input. Although inference based on a single tree can be misleading, the skyline plot uses the amount of genetic variation to estimate an independent population size for every interval between successive node heights in the tree, and is therefore useful for exploring more complex patterns of demographic history than is possible with the standard parametric models available in BEAST. In this case, the MAP tree resulting from the analysis using the constant population size Bayesian analysis was used as input. The close match of the Bayesian and skyline results indicate that phylogenetic uncertainty did not cause significant bias.

Each of the demographic models that were evaluated assumed a single panmictic population across the bison range. The migration observed between eastern and western Beringia and between Beringia and central North America supports the assumption that there were no long-term barriers to gene flow between these geographic regions. However, the phylogeographic structure of the MAP tree (Fig S2) suggests that some population structure did indeed exist, if only for the short-term. To test for the effect of population structure on the analysis, the best-fitting (two-epoch) model was run as above except (a) excluding the Eurasian bison and (b) excluding Eurasian bison and bison from central North America (Alberta, British Columbia, and the lower 48 US). The results of these analyses were consistent with the full analysis, indicating that the model is robust to violation of an assumption of panmixia (Table S3). This suggests that the strength of the data is in the most heavily sampled region, Eastern Beringia. However, it remains unclear how much population structure existed across the range of bison during the period covered in this analysis, or the duration of time in which barriers to gene flow existed. The results are therefore presented inclusive of all bison specimens available with finite radiocarbon dates, although the results relating to population size and the timing of the population crash are assumed to pertain to the eastern Beringian population. Because the majority of western Beringian specimens sampled have infinite radiocarbon dates, and

because very little information is available for the population living in central North America prior to the early Holocene, it is currently not possible to separately evaluate these populations.

If our demographic results are interpreted according to metapopulation theory, the peak around 37 ka BP would mark the end of a long-term increase in the overall size of the bison metapopulation and the culmination of genetic exchange between demes, and also define the total effective metapopulation size. Under this interpretation, the value at the intersect with the y-axis is the effective population size for each individual deme, and the ratio of this number to the peak (approximately 230 in this instance) is the total number of demes in the metapopulation. The phylogeographic structure in our trees suggests many fewer than 230 demes, with significant migration between the geographic regions following 32-42 ka BP (Fig. S2), and therefore reject a simple metapopulation-based interpretation of the observed demographic pattern.

To test for the robustness of our results to incomplete sampling, 4 additional analyses were performed in which 95 samples were chosen at random from the entire dataset of ancient and modern bison. The analyses were performed as above, except only one run of 30 million iterations was run for each subset, with the first 3 million iterations discarded as burn-in. Although power of the analyses was reduced by the limited data, the results were consistent with those of the full analysis, and each major clade from Fig. S2 was represented in the MAP trees (Fig. S5).

Supporting Text and Figures

(a.) Possible survival of Beringian bison to the near present

One of the specimens belonging to clade 4b (Fig. S2) appears to be much younger than the others, and suggests the survival of Beringian bison haplotypes to the near present. This sample (BS469) has been associated with two independent radiocarbon dates placing it at 50±75 ka BP (BGS-2054) and 305±24 ka BP (OxA-11988), and has been extracted and cloned twice, each time resulting in identical mitochondrial DNA sequences. This specimen originates from Banff National Park in Alberta, not far from the location of all other specimens in clade 4b, however was found ex-situ. The radiocarbon ages assigned to this specimen may be the result of contamination by modern bone material, and require further analysis. If the dates are correct, however, this specimen is the only evidence of a Beringian steppe bison mitochondrial haplotype surviving to the near present.

(b.) Analysis of 57 modern bison sequences:

To investigate the recent evolutionary history of extant bison, analyses were restricted to 57 individuals representing a strongly supported phylogenetic clade (subclade 1a; Fig. S2) including all modern bison sequences. Values for the transition/transversion ratio, proportion of invariant sites, and the gamma distribution were fixed to the mean values estimated in the full analysis, and the population demography and divergence times were co-estimated using MCMC. Two chains of 20 million iterations were run, with trees sampled every 1000 iterations. The first 1.5 million iterations were discarded from each chain and the remainder was combined. The analysis was performed assuming: a constant population size, exponential growth, and a two-epoch demographic model. Standard statistical tests(*S7*) were used to determine the model that best fit the data. The results of these three analyses are given in Table S4. Following the bottleneck at the MRCA, populations increase exponentially to a peak around 1000 years ago (range: 63-2300) and then rapidly decline. This signal is consistent with the known bottleneck of the 1880s, but it is interesting that the Holocene population increase occurred despite significant Native American hunting pressure(*S11*).

Previous nuclear and mitochondrial analyses have been unsuccessful in confirming a genetic basis for the distinct subspecific status of the wood and plains bison in North America(*S12, S13*). These results have been attributed to the introgression of plains bison DNA into wood bison populations in 1925, as part of conservation efforts. To confirm this, we included in our analyses three wood bison predating the 1925 introductions (Fig. S2a, light blue specimens). Although the sample size is small, these three specimens only form a monophyletic group in 3.7% of the observed posterior genealogies. Therefore, ancient DNA finds no support for the separate subspecific status of wood and plains bison, even prior to 1925.

Table S1: Detailed description of specimens. The following table describes each of the specimens used in this study, detailing the success of DNA amplification, whether the sample has been cloned and/or replicated, where the specimen is currently housed (and accession numbers where applicable), and details of where the specimen originated. Radiocarbon dates and accession numbers, or approximate ages of the specimens based on stratigraphic information, are also listed.

Abbreviations for museum locations are as follows:

ABC: Ancient Biomolecules Centre, Oxford, UK;
ADFG: Alaska Department of Fish and Game, Fairbanks, AK, USA
AMNH: American Museum of Natural History, New York, USA
BLM: Bureau of Land Management, Fairbanks, AK, USA
ChLM: Local Museum, Chersky, Russia
ChNRS: Northern Research Station, Cherskii, Russia
CMN: Canadian Museum of Nature, Gatineau, Quebec, Canada
KU: University of Kansas Museum of Natural History, Lawrence, KS, USA
IMNH: Idaho Museum of Natural History, Idaho, USA
MW: M. C. Wilson, private collection
PC: Private collection (Specific information available from authors on request)
PIN: Paleontological Institute, Moscow, Russia
PMA: Provincial Museum of Alberta, Edmonton, Alberta, Canada
SFU: Simon Fraser University, Vancouver, BC, Canada
UAF: University of Alaska, Fairbanks, AK, USA
Uvic: University of Victoria, Victoria, BC, Canada
VNHM: Vienna Natural History Museum, Vienna, Austria
YDFW: Yukon Department of Fisheries and Wildlife, Whitehorse, YT, Canada
YHR: Yukon Heritage Resources, Whitehorse, YT, Canada
ZIN: Zoological Institute, St. Petersburg, Russia
ZMIPAE: Zoological museum of Institute of Plant and Animal Ecology, Ekaterinburg, Russia

Extraction no.	DNA ampl.	Clon/Repl	Sample	Museum	Accn. No.	Location	Element	Age (uncorr.)	Rdcbn Accn. No.
BS099	Y (all)	C	Bison b. athabascae	CMN	CMN 8755	Salt R., Salt Prairie, AB	tissue	collected 1924	
BS100	Y (all)	C, R	Bison b. athabascae	CMN	CMN 4538	Fort Smith, AB	tissue	collected 1921	
BS102	Y (all)	C	Bison b. athabascae	CMN	CMN 10405	Murdoch Cr., Wood Bison NP, AB	tissue	collected 1928	
BS105	Y (all)	R	Bison	AMNH	A-144-9359	Ester Cr., Fairbanks, AK	metacarpal	23380±460	D. Guthrie
BS106	Y		Bison	AMNH	A-179-2059	Cripple Cr., Fairbanks, AK	metacarpal		
BS107	Y (all)	R	Bison	AMNH	A-100-7749	Ester Cr., Fairbanks, AK	metacarpal	19570±290	D. Guthrie
BS108	Y (all)		Bison	AMNH	A-169-3115	Lower Eldorado Cr., Fairbanks, AK	metacarpal	21020±360	D. Guthrie
BS109	Y (all)	R	Bison	AMNH	A-237-7970	Lower Gold Stream, Fairbanks, AK	metacarpal	20730±350	D. Guthrie
BS110	N		Bison	AMNH	A-100-1205	Gold Stream, Fairbanks, AK	metacarpal	>40300	D. Guthrie
BS111	Y (all)		Bison	AMNH	A-105-6641	Ester Cr., Fairbanks, AK	metacarpal	21580±370	D. Guthrie
BS112	Y (>2/3)		Bison	AMNH	A-219-8090	Engineer Cr., Fairbanks, AK	metacarpal	>41000	D. Guthrie
BS113	Y (all)		Bison	AMNH	A-179-2068	Cripple Cr., Fairbanks, AK	metacarpal		
BS114	Y (all)	R	Bison	AMNH	A-105-5396	Engineer Cr., Fairbanks, AK	metacarpal	>41,000	D. Guthrie
BS115	Y (all)	R	Bison	AMNH	A-105-5319	Engineer Cr., Fairbanks, AK	metacarpal	>39000	D. Guthrie
BS121	Y (all)		Bison	AMNH	A-112-6450	Ester Cr., Fairbanks, AK	metacarpal	19360±280	D. Guthrie
BS122	N	R	Bison	AMNH	A-209-4359	Lower Eldorado Cr., Fairbanks, AK	metacarpal	>38000	D. Guthrie
BS123	Y (all)		Bison	ADFG	RS-9201	Black R.. Yukon Flats, AK	l. femur	1730±60	Beta 62999
BS124	Y (all)		Bison	ADFG	RS-9200	Black R.. Yukon Flats, AK	skull	11900±70	Beta 67494
BS125	Y (all)	R	Bison	AMNH	A-160-6681	Ester Cr., Fairbanks, AK	metacarpal	27440±790	D. Guthrie
BS126	Y (all)	C	Bison	AMNH	A-112-3346	Upper Cleary Cr., Fairbanks, AK	metacarpal	19150±280	D. Guthrie
BS127	Y (all)	C, R	Bison	AMNH	A-206-2449	Cripple Cr., Fairbanks, AK	metacarpal	>41000	D. Guthrie
BS128	Y (>2/3)	C	Bison	AMNH	A-112-4458	Fox, AK	metacarpal		
BS129	Y (all)		Bison	SFU	24CH234	Fort Benton, MT	bone	<200	
BS130	Y (all)		Bison	UAF	UA-79-123-59	Porcupine R. Cave, AK	tibia	9000±250	Beta 18552
BS131	N		Bison	KU	KU 53361	Natural Trap Cave, WY	metapodial		
BS133	Y (all)	C, R	Bison	AMNH	A-174-3123	Lower Eldorado Cr., Fairbanks, AK	metacarpal	33880±1900	D. Guthrie
BS134	N		Bison	AMNH	A-219-8005	Engineer Cr., Fairbanks, AK	metacarpal	>44000	D. Guthrie
BS135	N		Bison	AMNH	A-628-5454	Fairbanks Cr., Fairbanks, AK	metacarpal	>41,000	D. Guthrie
BS136	Y (all)		Bison	AMNH	A-148-9635	Ester Cr., Fairbanks, AK	metapodial		
BS137	N	R	Bison	AMNH	A-179-2052	Cripple Cr., Fairbanks, AK	metacarpal	33300±1600	D. Guthrie
BS138	Y (>2/3)	C, R	Bison	AMNH	A-148-9294	Ester Cr., Fairbanks, AK	metacarpal	25310±580	D. Guthrie
BS139	Y		Bison	AMNH	FAM 46836	Fox, AK	metapodial	>41000	D. Guthrie
BS140	N		Bison	AMNH	A-269-6036	Goldstream, Fox, AK	metacarpal	>41000	D. Guthrie
BS141	N		Bison	CMN	CMN CR-71-3	Dawson City, YT	horncore		
BS143	Y (all)		Bison	CMN	CMN 35783	Cripple Hill, Dawson City, YT	metacarpal	>62000	OxA-11992
BS145	Y (all)		Bison	BLM	IK-98-528	Ikpikpuk R., North Slope, AK	humerus	12270±50	CAMS 53774
BS146	Y (all)		Bison	BLM	IK-98-027	Ikpikpuk R., North Slope, AK	metacarpal	11810±50	CAMS 53756
BS147	Y (all)		Bison	BLM	IK-98-1115	Ikpikpuk R., North Slope, AK	astralagus	28120±290	CAMS 53892
BS148	Y (all)		Bison	BLM	IK-98-303	Ikpikpuk R., North Slope, AK	bone		
BS149	Y (all)		Bison	BLM	IK-98-032	Ikpikpuk R., North Slope, AK	metacarpal	46100±2200	CAMS 53757
BS150	Y (all)		Bison	BLM	IK-98-343	Ikpikpuk R., North Slope, AK	humerus	10510±50	CAMS 53767
BS151	Y (all)		Bison	BLM	IK-98-401	Ikpikpuk R., North Slope, AK	metacarpal	21530±130	CAMS 53770
BS161	Y (all)		Bison	BLM	IK-98-1090	Ikpikpuk R., North Slope, AK	astralagus	21040±120	CAMS 53890
BS162	Y (all)		Bison	UAF	No # (Guthrie)	Anchorage, AK	skull	170±30	Beta 136732
BS163	Y (all)		Bison	UAF	V-54-1157	Lost Chicken Cr., Chicken, AK	tibia	13240±75	OxA-10543
BS164	Y (all)		Bison	UAF	V-54-1099	Lost Chicken Cr., Chicken, AK	humerus	19540±120	OxA-11139

BS165	Y (all)	C, R	Bison	UAF	V-54-60	Lost Chicken Cr., Chicken, AK	radius	26460±160	OxA-11131
BS166	Y (all)		Bison	UAF	B1.07.B3	Lost Chicken Cr., Chicken, AK	bone		
BS167	Y (all)		Bison	UAF	B1.07.B2	Lost Chicken Cr., Chicken, AK	bone		
BS170	Y (all)		Bison	CMN	CMN 46699	Bison Cave, Fishing Branch, YT	metatarsal	13040±70	OxA-10681
BS171	Y (all)	C, R(3)	Bison	UAF	A-191	Chalkyitsik, AK	skull	4390±70	Beta 136731
BS172	Y (all)		Bison	UAF	V-54-1105	Lost Chicken Cr., Chicken, AK	metapodial	12525±70	OxA-10541
BS173	Y (all)		Bison	KU	KU 42887	Natural Trap Cave, WY	metapodial	3220±45	OxA-11271
BS174	N		Bison	SFU	290	Fort Benton, MT	bone	<2000	
BS175	Y (all)		Bison	KU	KU 23002	Ice Cave, MT	metapodial	186±30	OxA-11195
BS176	Y (all)		Bison	UAF	V-54-365	Lost Chicken Cr., Chicken, AK	tibia	12380±60	OxA-11226
BS177	Y (all)		Bison	KU	KU 44361	Natural Trap Cave, WY	metapodial	3155±36	OxA-11169
BS178	Y (all)		Bison	UAF	V-54-1137	Lost Chicken Cr., Chicken, AK	tibia	17960±90	OxA-10542
BS192	Y (all)		Bison	BLM	P-013	Palisaides, AK	metatarsal	26300±300	Beta 110938
BS193	Y (all)	C	Bison	BLM	IK-98-928	Ikpikpuk R., North Slope, AK	astralagus	49600±4000	CAMS 53783
BS195	Y (all)		Bison	BLM	IK-98-616	Ikpikpuk R., North Slope, AK	metacarpal	29040±340	CAMS 53775
BS196	Y (all)		Bison	BLM	IK-98-504	Ikpikpuk R., North Slope, AK	femur	19420±100	CAMS 53772
BS197	Y (all)		Bison	BLM	IK-98-218	Ikpikpuk R., North Slope, AK	astralagus	>46600	CAMS 53762
BS198	Y (all)		Bison	YDFW		Braeburn, YT	skull	2460±40	Beta 137731
BS199	Y (all)		Bison	SFU	3894	Fort D'Epinette, Peace R., BC	radius		
BS200	Y (all)		Bison	SFU	6584	Fort D'Epinette, Peace R., BC	metapodial	145±37	OxA-10579
BS201	Y (all)		Bison	CMN	CMN 46695	Dawson City, YT	humerus	12960±60	OxA-11197
BS202	Y (all)		Bison	UVic	#1 Williston L.	Fort D'Epinette, Peace R., BC	metapodial	10460±65	OxA-11272
BS205	Y (all)		Bison	ChNRS	CRS-SY-12	Kolyma lowland, Stanchikovsky Yar, Siberia	metatarsal	42150±650	OxA-11333
BS206	Y (all)		Bison	ChNRS	CRS-IC-30	Kolyma lowland, Bol. Khomus-Yuryakh R., Siberia	skull	23780±140	OxA-11194
BS208	Y (all)		Bison	ChNRS	CRS-DY-12	Kolyma lowland, Duvanny Yar, Siberia	vertebra	>65200	OxA-11198
BS209	Y (all)		Bison	ChLM	CRS-DY-43	Kolyma lowland, Duvanny Yar, Siberia	tibia	>57700	OxA-11192
BS210	Y (all)		Bison	ChNRS	CRS-SY-210	Kolyma lowland, Stanchikovsky Yar, Siberia	bone		
BS211	Y (all)		Bison	ChNRS	CRS-IC-5	Kolyma lowland, Bol. Khomus-Yuryakh R., Siberia	metapodial	43800±1100	OxA-10577
BS212	Y (all)	C	Bison	ChNRS	CRS-SY-2	Kolyma lowland, Stanchikovsky Yar, Siberia	metacarpal	>55600	OxA-10575
BS213	Y (all)		Bison	ChNRS	CRS-IC-26	Kolyma lowland, Bol. Khomus-Yuryakh R., Siberia	ulna	>56800	OxA-11225
BS214	Y (all)		Bison	ChLM	CRS-DY-36	Kolyma lowland, Duvanny Yar, Siberia	scapula	>58,000	OxA-10578
BS216	Y (all)	R	Bison	BLM	IK-98-671	Ikpikpuk R., North Slope, AK	metacarpal	47000±2900	CAMS 53778
BS218	Y (all)		Bison	PIN	PIN 3916-113-24	Kolyma lowland, Alyoshkina Zaimka, Siberia	tibia	14605±75	OxA-11140
BS219	Y (all)		Bison	UAF	AK-277-V-34	Ikpikpuk R., North Slope, AK	femur		
BS222	Y (all)		Bison	CMN	CMN 12087	Baillie Island, NWT	bone	6110±45	OxA-11165
BS223	Y (all)		Bison	PIN	BL-0193-15-R	Novosibirsk Islands, Zimovye R., Siberia	vertebra	53300±1900	OxA-11130
BS224	Y (all)		Bison	AMNH	A-93-8430	Chatanika, AK	metatarsal	13125±75	OxA-11277
BS225	N		Bison pre-occidentalis	AMNH	A-437-1348	Upper Redrow Cr., AK	skull		
BS228	N	R	Bison	UAF	V-11-4	Central, AK	vertebra		

BS230	N		Bison	SFU	16410	Charlie Lake Cave, Peace R., BC	radius		
BS231	N		Bison	CMN	CMN 38467	Maitland. NWT	bone		
BS232	N		Bison	CMN	CMN 25267	Eskimo Lakes, NWT	tarsus		
BS233	Y (all)		Bison	UAF	V-16-28	Elephant Point, AK	humerus	16685±80	OxA-11223
BS234	N		Bison	UAF	V-54-13	Lost Chicken Cr., Chicken, AK	femur		
BS235	Y (all)		Bison	UAF	No # (BSX2)	Yukon R., AK	skull	43400±900	OxA-11163
BS236	Y (all)		Bison	AMNH	FAM 32761	Seward Pininsula, Alder Cr., AK	femur	19420±100	OxA-11247
BS237	Y (all)	C, R	Bison	UVic	#2, E. Pine gp	Chetwynd, BC	humerus	11240±70	OxA-11274
BS241	N	R	Bison	UVic	No #	McCulloch Station, BC	vertebrae		
BS242	Y (>2/3)	C, R	Bison	AMNH	FAM 14332	Eschscholtz Bay, AK	metacarpal	53800±2900	OxA-11273
BS243	Y (all)		Bison	AMNH	FAM 14344	Seward Pininsula, Alder Cr., AK	horncore	37550±400	OxA-11196
BS244	Y (all)		Bison	UAF	V-54-29	Lost Chicken Cr., Chicken, AK	metapodial	26210±170	OxA-11227
BS245	Y (all)		Bison	AMNH	A-160-7764	Ester Cr., Fairbanks, AK	metacarpal		
BS246	Y (all)		Bison	UAF	V-54-1088	Lost Chicken Cr., Chicken, AK	r. ulna	13160±70	OxA-10540
BS247	Y (all)		Bison	UAF	V-54-712	Lost Chicken Cr., Chicken, AK	metapodial	>55800	OxA-10539
BS248	Y (all)		Bison	CMN	CMN 33039	Old Crow, YT	skull	12350±70	OxA-10546
BS249	Y (all)	C, R	Bison pre-occidentalis	AMNH	A-606-1082	Fairbanks Cr., Fairbanks, AK	skull	39200±550	OxA-10683
BS250	Y (>2/3)	C	Bison	AMNH	A-678-3133	Dome Cr., Fairbanks, AK	femur	>56000	OxA-10685
BS251	N		Bison	ADFG	RS-9801	Black R.. Yukon Flats, AK	humerus		
BS252	Y (>2/3)	C	Bison	CMN	CMN 34726	Gold Run Cr., Dawson City, YT	metacarpal	21500±130	OxA-10547
BS253	Y (all)		Bison	UAF	V-54-677	Lost Chicken Cr., Chicken, AK	humerus	12665±65	OxA-10855
BS254	Y (all)	C	Bison	SFU	20043	Charlie Lake Cave, Peace R., BC	tibia	10230±55	OxA-10580
BS255	Y (>2/3)		Bison	CMN	CMN 42113	Boliden Cr., Carmacks, YT	metacarpal	>56,000	OxA-10548
BS256	Y (all)	C	Bison	UAF	V-54-17	Lost Chicken Cr., Chicken, AK	tibia	12340±65	OxA-10679
BS257	Y (all)		Bison	CMN	CMN 47439	Last Chance Cr., Dawson City, YT	metacarpal	>57500	OxA-10682
BS258	Y (all)		Bison	UAF	Ak-316-V-11	Fairbanks Cr., Fairbanks, AK	scapula	22120±130	OxA-10581
BS259	Y (all)	C	Bison	UAF	V-54-226	Lost Chicken Cr., Chicken, AK	femur	12960±70	OxA-10538
BS260	Y (all)	C, R	Bison	CMN	CMN 49583	Quartz Cr., Dawson City, YT	metacarpal	30750±290	OxA-10574
BS261	Y (all)		Bison	CMN	CMN 25856	Lost Chicken Cr., Chicken, AK	metatarsal	12915±70	OxA-10544
BS262	Y (all)		Bison	CMN	CMN 35365	Hunker Cr., Dawson City, YT	metatarsal	29150±500	OxA-10680
BS270	Y		Bison	YDFW	FR-00-15	Friday Cr., Whitehorse, YT	faeces	modern	
BS272	Y	C	Bison	YDFW	Fri-99-19	Frick, YT	faeces	modern	
BS279	Y (all)	C	Bison	PIN	MKh-01-420	Lena R. Delta, Bykovsky Pen., Siberia	femur	>59300	OxA-11167
BS280	Y	C	Bison	CMN	CMN 45289	Hunker Cr., Dawson City, YT	tissue		
BS281	Y (all)		Bison	ADFG	RS-0104	Black R.. Yukon Flats, AK	humerus	40800±600	OxA-11275
BS282	Y (all)		Bison	PIN	MKh-01-467	Lena R. Delta, Bykovsky Pen., Siberia	metatarsal	56700±3200	OxA-11278
BS283	Y (all)		Bison	UAF	IK-01-262	Ikpikpuk R., North Slope, AK	bone		
BS284	Y (all)		Bison	CMN	CMN 46696	Bison Cave, Fishing Branch, YT	humerus	13135±65	OxA-11166
BS285	Y (all)	C	Bison	UAF	V-37-30	Sheep Cr., Fairbanks, AK	skull	>5900	OxA-11279
BS286	Y (all)		Bison	PIN	MKh-01-465	Lena R. Delta, Bykovsky Pen., Siberia	tibia	49500±1300	OxA-11135
BS287	Y (all)		Bison	ADFG	RS-0102	Black R.. Yukon Flats, AK	humerus	49100±1700	OxA 11164
BS288	Y (>2/3)		Bison	UAF	VA-97-061-229	Gerstle R., near Fairbanks, AK	astralagus	9400±55	OxA-11246
BS289	Y (all)	C	Bison	ADFG	RS-0105	Black R.. Yukon Flats, AK	bone	2172±37	OxA-11248
BS291	Y (all)		Bison	UAF	IK-01-216	Ikpikpuk R., North Slope, AK	metatarsal	49700±1400	OxA-11136
BS292	Y (all)		Bison	BLM	IK-98-916	Ikpikpuk R., North Slope, AK	astralagus	35710±730	CAMS 53782

BS293	Y (all)		Bison	ChNRS	CRS-IC-32	Kolyma lowland, Bol. Khomus-Yuryakh R., Siberia	skull	>58800	OxA-11132
BS294	Y (all)		Bison	ADFG	RS-0103	Black R.. Yukon Flats, AK	humerus	58200±3900	OxA-11276
BS295	N		Bison	CMN	CMN 47476	Oro Grande Cr., Dawson City, YT	metacarpal	>47,500	OxA-10573
BS296	Y (all)		Bison	UAF	V-54-55	Lost Chicken Cr., Chicken, AK	metacarpal	24950±170	OxA-10537
BS297	Y (all)	C	Bison	BLM	IK-98-1114	Ikpikpuk R., North Slope, AK	astralagus	10990±50	CAMS 53891
BS298	N		Bison	ChNRS	CRS-CB-1	Kolyma lowland, Chersky, Siberia	humerus		
BS299	Y (all)		Bison	ChNRS	CRS-IC-18	Kolyma lowland, Bol. Khomus-Yuryakh R., Siberia	metapodial	>56800	OxA-11921
BS301	Y (all)		Bison	CMN	CMN 44404	Hunker Cr., Dawson City, YT	metacarpal	>56800	OxA-11168
BS303	Y (all)		Bison	ChLM	CRS-DY-41	Kolyma lowland, Duvanny Yar, Siberia	radius/ulna		
BS304	Y (all)		Bison	ChNRS	CRS-SY-13	Kolyma lowland, Stanchikovsky Yar, Siberia	ulna	>63200	OxA-11956
BS305	Y (all)		Bison	AMNH	A-139-6008	Ester Cr., Fairbanks, AK	metapodial		
BS306	Y (all)	C	Bison	ChNRS	CRS-IC-16	Kolyma lowland, Duvanny Yar, Siberia	metapodial		
BS307	Y (all)	C	Bison alaskensis	AMNH	A-424-1259	Ester Cr., Fairbanks, AK	skull		
BS308	Y (all)	C, R	Bison pre-occidentalis	AMNH	A-251-7922	Lower Gold Stream, Fairbanks, AK	skull		
BS309	Y (all)	C	Bison	ChNRS	CRS-IC-17	Kolyma lowland, Omolon R., Siberia	metapodial		
BS310	Y (all)		Bison	ChNRS	CRS-SY-11	Kolyma lowland, Stanchikovsky Yar, Siberia	metacarpal		
BS311	Y (all)	C	Bison	ADFG	RS-9901	Black R.. Yukon Flats, AK	humerus	12425±45	OxA-12067
BS312	Y	C, R	Bison	UAF	V-16-33	Elephant Point, AK	radius		
BS313	Y (all)	C, R	Bison	ChLM	CRS-DY-42	Kolyma lowland, Duvanny Yar, Siberia	metacarpal		
BS314	Y (all)		Bison	PIN	BL-0242-R	Novosibirsk Islands, Zimovye R., Siberia	radius	>59100	OxA-11134
BS315	N		Bison	UAF	VA-2000-54-77	Gerstle R., near Fairbanks, AK	astralagus	8960±70	
BS316	Y (all)		Bison	ChNRS	CRS-IC-19	Kolyma lowland, Omolon R., Siberia	metapodial	57700±3000	OxA-12070
BS318	Y (all)		Bison	BLM	IK-98-142	Ikpikpuk R., North Slope, AK	metatarsal	12410±50	CAMS 53760
BS320	Y (all)		Bison	ChNRS	CRS-IC-28	Kolyma lowland, Duvanny Yar, Siberia	metapodial	49600±1500	OxA-11133
BS321	Y (all)		Bison	UAF	XMH-246	Gerstle R., near Fairbanks, AK	metatarsal	9506±38	OxA-11962
BS323	Y (all)		Bison	PIN	BL-0722-L	Novosibirsk Islands, Zimovye R., Siberia	metacarpal	37810±380	OxA-11224
BS324	Y (all)	C	Bison	UAF	V-54-621	Lost Chicken Cr., Chicken, AK	tibia		
BS325	Y (all)		Bison	BLM	IK-98-1167	Ikpikpuk R., North Slope, AK	astralagus	>49,900	CAMS 53898
BS326	Y (all)	C, R	Bison	ChNRS	CRS-IC-29	Kolyma lowland, Bol. Khomus-Yuryakh R., Siberia	radius/ulna	>57300	OxA-10576
BS327	Y (all)		Bison	CMN	CMN 49764	Eldorado Cr., Dawson City, YT	metacarpal	31530±230	OxA-11137
BS328	Y (all)	C, R	Bison	ChNRS	CRS-IC-4	Kolyma lowland, Duvanny Yar, Siberia	tibia	31690±180	OxA-12088
BS329	Y (all)		Bison	CMN	CMN 49692	Hester Cr., Dawson City, YT	metacarpal	27060±190	OxA-11193
BS330	Y (all)	C	Bison	ADFG	RS-0106	Black R.. Yukon Flats, AK	horncore		
BS331	Y (all)	R	Bison	ChLM	CRS-DY-39	Kolyma lowland, Duvanny Yar, Siberia	scapula	>62600	OxA-12069
BS333	N		Bison geisti	AMNH	A-580-2006	Fairbanks Cr., Fairbanks, AK	skull		

BS334	N		Bison alaskensis	AMNH	A-421-1216	Engineer Cr., Fairbanks, AK	skull		
BS335	N		Bison pre-occidentalis	AMNH	A-605-3002	Dome Cr., Fairbanks, AK	skull		
BS336	Y		Bison geisti	AMNH	FAM 30552	Cleary Cr., Fairbanks, AK	skull		
BS337	Y (all)	C	Bison	SFU	1848	Charlie Lake Cave, Peace R., BC	humerus		
BS338	Y (>2/3)		Bison pre-occidentalis	AMNH	FAM 30567	Cleary Cr., Fairbanks, AK	skull		
BS339	N		Bison geisti	AMNH	FAM 46893	Cripple Cr., Fairbanks, AK	skull		
BS340	Y (all)		Bison	BLM	IK-98-302	Ikpikpuk R., North Slope, AK	radius	24500±180	CAMS 53764
BS341	N		Bison geisti	AMNH	FAM 30581	Cleary Cr., Fairbanks, AK	skull		
BS342	Y (all)	C	Bison	SFU	2294	Charlie Lake Cave, Peace R., BC	radius	10340±40	OxA-12084
BS343	Y (all)	C	Bison	KU	KU 43556	Natural Trap Cave, WY	metatarsal		
BS344	N		Bison	KU	KU 61712	Natural Trap Cave, WY	bone		
BS345	Y (all)		Bison	BLM	IK-98-915	Ikpikpuk R., North Slope, AK	astralagus	39800±1200	CAMS 53781
BS346	Y	C	Bison	KU	KU 126033	Rawlins County, KS	bone		
BS348	Y (all)	C	Bison	SFU	16422	Charlie Lake Cave, Peace R., BC	carpal	10505±45	OxA-12085
BS349	N		Bison	KU	KU 126060	Rawlins County, KS	bone		
BS350	Y (all)		Bison	BLM	IK-98-377	Ikpikpuk R., North Slope, AK	astralagus	38700±1000	CAMS 53769
BS351	Y (all)	C	Bison	ADFG	RS/BSX1	Black R.. Yukon Flats, AK	radius	57700±3200	OxA-11138
BS352	N		Bison	KU	KU 50992	Natural Trap Cave, WY	metatarsal		
BS353	Y (all)	C	Bison	ChNRS	CRS-SY-3	Kolyma lowland, Stanchikovsky Yar, Siberia	humerus		
BS354	Y (all)		Bison	UAF	VA-97-061-21	Gerstle R., near Fairbanks, AK	metacarpal		
BS355	N		Bison	SFU	13730	Charlie Lake Cave, Peace R., BC	phalange		
BS356	Y (>2/3)		Bison	CMN	CMN 45517	Maisy May Cr., Dawson City, YT	metacarpal		
BS358	N		Bison	KU	KU 61546	Natural Trap Cave, WY	bone		
BS359	Y (all)	C	Bison	KU	KU 26057	Natural Trap Cave, WY	metatarsal	20020±150	OxA-12068
BS360	Y (all)	C	Bison	ChLM	CRS-DY-38	Kolyma lowland, Duvanny Yar, Siberia	metapodial	>58,000	OxA-10578
BS361	N		Bison	KU	KU 126018	Rawlins County, KS	bone		
BS363	N		Bison	CMN	CMN 47892-B	Old Crow, YT	metacarpal		
BS364	Y (>2/3)		Bison	BLM	IK-98-889	Ikpikpuk R., North Slope, AK	astralagus	38800±1100	CAMS 53779
BS366	N		Bison	CMN	CMN 33923	Hunker Cr., Dawson City, YT	metacarpal		
BS367	Y (>2/3)		Bison	CMN	CMN 50159	Oro Grande, Dawson City, YT	metacarpal		
BS368	Y (all)		Bison	SFU	No # (Ind #2)	Fort Benton, MT	bone	<200	
BS369	Y (>2/3)		Bison	CMN	CMN 44495	Bonanza Cr., Dawson City, YT	metacarpal		
BS370	Y		Bison	CMN	CMN 49828	Quartz Cr., Dawson City, YT	metacarpal		
BS371	Y (>2/3)		Bison	CMN	CMN 47185	Quartz Cr., Dawson City, YT	metacarpal		
BS372	Y (all)		Bison	CMN	CMN 45653	Gold Run Cr., Dawson City, YT	metacarpal		
BS373	Y (all)	C	Bison	CMN	CMN 33037	Old Crow, YT	skull		
BS375	Y (all)	C	Bison	CMN	CMN 47414	Independence Cr., Dawson City, YT	metacarpal		
BS376	Y (>2/3)	C	Bison	CMN	CMN 46347	Eldorado Cr., Dawson City, YT	metacarpal		
BS377	Y (>2/3)		Bison	CMN	CMN 47551	Last Chance Cr., Dawson City, YT	metacarpal	28850±220	OxA-11626
BS378	Y (all)		Bison	CMN	CMN 35270	Hunker Cr., Dawson City, YT	metacarpal		
BS379	Y		Bison	CMN	CMN 35259	Hunker Cr., Dawson City, YT	metacarpal		
BS380	Y (>2/3)		Bison	AMNH	A-332-2681	Cripple Cr., Fairbanks, AK	metatarsal		
BS381	Y (>2/3)		Bison	CMN	CMN 49872	Hester Cr., Dawson City, YT	metacarpal		
BS383	Y		Bison	CMN	CMN 29088	Quartz Cr., Dawson City, YT	metacarpal		

BS384	N		Bison	CMN	CMN 35890	Hunker Cr., Dawson City, YT	metatarsal		
BS385	Y (>2/3)		Bison	CMN	CMN 35891	Hunker Cr., Dawson City, YT	metacarpal	26760±120	OxA-12087
BS387	Y (all)		Bison	BLM	IK-98-1323	Ikpikpuk R., North Slope, AK	femur	33320±540	CAMS 53903
BS388	Y (all)		Bison	BLM	IK-98-374	Ikpikpuk R., North Slope, AK	metacarpal	27590±280	CAMS 53768
BS389	Y (all)		Bison	BLM	IK-98-661	Ikpikpuk R., North Slope, AK	metapodial	17160±80	CAMS 53777
BS390	Y (all)		Bison	BLM	IK-98-096	Ikpikpuk R., North Slope, AK	radius	31630±440	CAMS 53759
BS391	Y (all)	C	Bison	BLM	IK-98-1041	Ikpikpuk R., North Slope, AK	tibia	>48,500	CAMS 53886
BS392	Y (all)		Bison	BLM	IK-98-1222	Ikpikpuk R., North Slope, AK	metacarpal	36320±780	CAMS 53900
BS393	Y (all)		Bison	BLM	IK-98-174	Ikpikpuk R., North Slope, AK	astralagus	39850±1200	CAMS 53761
BS394	Y (all)		Bison	BLM	IK-98-1120	Ikpikpuk R., North Slope, AK	metacarpal	37460±890	CAMS 53893
BS395	Y (all)		Bison	BLM	IK-98-1122	Ikpikpuk R., North Slope, AK	metacarpal	40700±1300	CAMS 53895
BS396	Y (all)		Bison	BLM	IK-98-1254	Ikpikpuk R., North Slope, AK	femur	23680±170	CAMS 53901
BS397	Y (all)		Bison	BLM	IK-98-1035	Ikpikpuk R., North Slope, AK	humerus	32370±470	CAMS 53885
BS398	Y (all)		Bison	BLM	IK-98-095	Ikpikpuk R., North Slope, AK	radius	27400±260	CAMS 53758
BS399	Y (all)	C	Bison	BLM	IK-98-1299	Ikpikpuk R., North Slope, AK	metapodial	>49,500	CAMS 53902
BS400	Y (all)		Bison	BLM	IK-98-305	Ikpikpuk R., North Slope, AK	radius	46100±2600	CAMS 53766
BS402	Y (all)	C, R	Bison	UAF	#29 (UAF)	Elephant Point, AK	skull		
BS403	Y (all)	C	Bison	YHR	30.2	Revenue Cr., Dawson City, YT	metacarpal	>51200	OxA-11683
BS404	Y (all)	C	Bison	ZIN	StP-2	Yana-Indigirka lowland, Siberia	humerus	>56100	OxA-11628
BS405	Y (all)		Bison	ZIN	StP-7	Yana-Indigirka lowland, Siberia	tibia	23040±120	OxA-11629
BS406	Y (>2/3)	C	Bison pre-occidentalis	AMNH	A-382-4655	Cripple Cr., Fairbanks, AK	skull		
BS407	Y (all)		Bison	CMN	CMN 21096	Eskimo Lakes, NWT	bone	55500±3100	OxA-11630
BS408	Y (all)		Bison	ZIN	StP-1	Yana-Indigirka lowland, Siberia	tibia	>54100	OxA-12027
BS409	N		Bison	UAF	V-66	Fairbanks, AK	tibia		
BS410	Y (all)	C, R	Bison	YHR	36.2	Whitehorse, YT	metatarsal		
BS411	Y (all)	C, R	Bison	UAF	V-16-30	Elephant Point, AK	femur		
BS412	Y (all)		Bison	YHR	3.124	Finning, Whitehorse, YT	metatarsal	30500±250	OxA-11280
BS413	Y (all)		Bison	ZIN	StP-6	Yana-Indigirka lowland, Siberia	tibia		
BS414	Y (all)		Bison	ADFG	RS-9202	Black R.. Yukon Flats, AK	skull	4495±60	Beta 65662
BS415	Y (all)		Bison	CMN	CMN 46320	Nugget Gulch, Dawson City, YT	skull	30810±975	Beta 33192
BS417	Y (all)		Bison	PMA	572R30E6-2	Waterton Lakes NP, AB	tibia	909±29	OxA-11590
BS418	Y (all)	C, R	Bison	PMA	ASA-D91-37	Yanjiagang site, Harbin, China	femur	26560±670	AECV:1402c
BS419	Y (all)		Bison	PMA	47 T 10	Tuscany Site, Calgary, AB	femur	7475±45	OxA-11622
BS421	Y (all)		Bison	PMA	Unit27 Level T	Stampede Site, Cypress Hills, AB	radius	8145±45	OxA-11577
BS422	Y (all)		Bison occidentalis	PMA	P00.1.12	Byrtus Site, Athabasca, AB	metacarpal	908±31	OxA-11627
BS423	Y (all)		Bison	PMA	Unit14 Level V	Stampede Site, Cypress Hills, AB	bone	4660±38	OxA-11579
BS424	Y (all)		Bison occidentalis	PMA	P02.1.1	Fort Vermilion, AB	humerus	202±32	OxA-11625
BS425	Y		Bison occidentalis	PMA	P69.17.19	Duffield Site, AB	skull	6400±400	OxA-11586
BS426	Y (all)		Bison	PMA	12 Q 62	Stampede Site, Cypress Hills, AB	metatarsal	7060±45	OxA-11589
BS427	N		Bison	PMA	PMA, AA63/24	Old Womens Buffalo Jump, AB	metatarsal		
BS428	Y (all)		Bison	PMA	30 O 1	Stampede Site, Cypress Hills, AB	metatarsal	7105§±45	OxA-11581
BS429	Y (all)		Bison	PMA	17 R 9	Tuscany Site, Calgary, AB	metatarsal	6775±40	OxA-11585
BS430	Y (>2/3)		Bison occidentalis	PMA	UA No. 600	Cloverbar Pit, Edmonton, AB	skull	9270±50	OxA-11588
BS432	Y (all)		Bison	PMA	41 Q 1	Tuscany Site, Calgary, AB	metacarpal	7310±45	OxA-11583

BS433	Y (all)		Bison occidentalis	PMA	P00.1.4	Byrtus Site, Athabasca, AB	humerus	10450±55	OxA-11584
BS434	Y (all)	C	Bison	PMA	P68.2.1039	Boss Hill Arch site, Stettler, AB	radius	809±32	OxA-11623
BS435	N		Bison	PMA	P94.1.673	Cons. Pit 48, Edmonton, AB	humerus		
BS436	Y (>2/3)	C	Bison	PMA	88-29:13668	Fletcher Site	metatarsal		
BS437	Y	C	Bison	PMA	P68.2.1077	Boss Hill Arch site, Stettler, AB	tibia	693±33	OxA-11578
BS438	Y (>2/3)	C	Bison	PMA	P94.1.201	Cons. Pit 48, Edmonton, AB	mandible	53800±2200	OxA-11620
BS439	Y (all)	C	Bison occidentalis	PMA	P80.42.1	Horse Hills Pit, Edmonton, AB	skull	5845±45	OxA-11624
BS440	Y (all)	C, R	Bison	PMA	P89.13.692	Cons. Pit 48, Edmonton, AB	metatarsal	60400±2900	OxA-12086
BS441	Y (all)		Bison	PMA	572R30G-2	Waterton Lakes NP, AB	metatarsal	1273±32	OxA-11591
BS442	Y		Bison	PMA	PMA, AA63/62	Old Womens Buffalo Jump	metacarpal	9510±55	OxA-11612
BS443	Y (all)		Bison	PMA	P94.1.932	Cons. Pit 48, Edmonton, AB	metacarpal	34050±450	OxA-11613
BS444	Y (all)		Bison	PMA	P85.13.1	Edmonton, AB	mandible	636±29	OxA-11582
BS445	Y (all)	C	Bison	PMA	1326R100A1-1	Banff NP, AB	mandible	378±30	OxA-11593
BS447	N		Bison	UAF	NO #	Fairbanks, AK	bone		
BS449	Y (>2/3)	C, R	Bison	PMA	L EE31 No. 21068	Stampede Site, Cypress Hills, AB	humerus	6195±45	OxA-11621
BS451	N		Bison	PMA	87-55, 3023-3047	Fletcher Site	tibia		
BS452	Y (all)		Bison	PMA	P89.13.693	Cons. Pit 48, Edmonton, AB	metat	>55200	OxA-11611
BS453	N		Bison	PMA	87-55:2877	Fletcher Site	metatarsal		
BS454	Y (all)		Bison	PMA	1797R1A1-1	Panther R., Banff NP, AB	skull	287±29	OxA-11587
BS455	Y (all)		Bison	PMA	P95.2.87	Apex-Evergreen, Edmonton, AB	radio/ulna	>59400	OxA-11616
BS456	Y (all)	C	Bison	PMA	P68.2.1052	Boss Hill Arch site, Stettler, AB	humerus	125±30	OxA-11580
BS457	Y (all)		Bison	PMA	P99.3.44	Cons. Pit 48, Edmonton, AB	radius	>52600	OxA-11609
BS458	Y (all)	C	Bison	UAF	V-51-4	Chena R., Fairbanks, AK	metapodial		
BS459	Y (all)	C	Bison	PMA	HY85-299	Yanjiagang site, Harbin, China	metacarpal	47700±1000	OxA-11634
BS460	Y (all)		Bison occidentalis	PMA	P00.1.11	Byrtus Site, Athabasca, AB	metacarpal	10425±50	OxA-11592
BS462	Y		Bison	PMA	P94.8.55	Riverview Pit, Edmonton, AB	tibia	>58500	OxA-11619
BS463	N		Bison	PMA	P89.13.255	Cons. Pit 48, Edmonton, AB	horncore	40000±3070	AECV:1664c
BS464	Y (all)		Bison	PMA	P96.10.34	Edmonton, AB	metacarpal	5205±45	OxA-11610
BS465	Y (all)	C	Bison	PMA	Unit9 Level A	Stampede Site, Cypress Hills, AB	astralagus	7115±50	OxA-11614
BS466	Y (all)		Bison occidentalis	PMA	P79.26.1	Llyodminster, AB	skull	3298±37	OxA-11618
BS467	Y (>2/3)		Bison	PMA	P89.14.16	Cloverbar Pit, Edmonton, AB	horncore	>41,800	AECV:1862c
BS468	Y (all)		Bison	UAF	V-15-153	Dome Cr., Fairbanks, AK	scapula		
BS469	Y (all)	C, R	Bison	PMA	1912R1A1-8	Banff National Park, AB	mandible	50±75, 305±24	BGS-2054, OxA-11988
BS470	N		Bison	PMA	ASA-D91-44	Tong He, China	humerus		
BS471	Y (>2/3)		Bison	PMA	88-29:416	Fletcher Site, AB	bone		
BS472	Y (all)		Bison	AMNH	A-556-4160	Fairbanks Cr., Fairbanks, AK	metatarsal	13235±65	OxA-11617
BS473	Y (all)		Bison	PMA	P95.12.2	Twin Bridges Gravel Pit, AB	femur	56300±3100	OxA-11615
BS474	Y (all)	C	Bison	AMNH	A-691-2211	Fairbanks Cr., Fairbanks, AK	femur		
BS475	N		Bison	PMA	P90.6.072	Apex Evergreen, Edmonton, AB	humerus		
BS477	Y (all)		Bison	ABC	110.20a	Evergreen Cr., Dawson City, YT	humerus	33710±240	OxA-11960
BS478	Y (all)		Bison	ABC	110.19	Evergreen Cr., Dawson City, YT	humerus	34470±200	OxA-11991
BS479	Y (all)		Bison	ABC	110.12	Evergreen Cr., Dawson City, YT	humerus		
BS480	Y (all)		Bison	ABC	110.18	Evergreen Cr., Dawson City, YT	humerus		
BS481	Y (all)		Bison	ABC	110.4	Evergreen Cr., Dawson City, YT	humerus		

BS488	Y (>2/3)		Bison	CMN	CMN 35357	Hunker Cr., Dawson City, YT	metacarpal	29200±210	OxA-11632
BS489	Y (>2/3)		Bison	CMN	CMN 35639	Eldorado Cr., Dawson City, YT	metacarpal		
BS490	Y (all)		Bison	ADFG	RS-0201	Birch Cr., Yukon Flats, AK	horncore	2415±25	OxA-11990
BS493	Y (all)	C	Bison	BLM	IK-98-527	Ikpikpuk R., North Slope, AK	vertebra	50000±4200	CAMS 53773
BS494	Y (>2/3)		Bison	BLM	IK-98-1042	Ikpikpuk R., North Slope, AK	ulna	44800±2200	CAMS 53887
BS495	Y (all)		Bison	BLM	IK-98-1164	Ikpikpuk R., North Slope, AK	metacarpal	29570±340	CAMS 53897
BS496	Y (all)		Bison	BLM	IK-98-863	Ikpikpuk R., North Slope, AK	astralagus	36520±800	CAMS 53914
BS497	Y (all)		Bison	BLM	IK-98-430	Ikpikpuk R., North Slope, AK	metapodial	30000±540	CAMS 53771
BS498	Y (all)	C	Bison	BLM	IK-98-1184	Ikpikpuk R., North Slope, AK	horncore	25980±230	CAMS 53899
BS499	Y (all)		Bison	BLM	IK-98-256	Ikpikpuk R., North Slope, AK	metapodial	31412±420	CAMS 53763
BS500	Y (all)		Bison	BLM	IK-98-1211	Ikpikpuk R., North Slope, AK	metacarpal	35580±550	CAMS 53894
BS501	Y (all)	C	Bison	CMN	CMN 49582	Quartz Cr., Dawson City, YT	metacarpal		
BS502	Y (all)		Bison	CMN	CMN 46324	Nugget Gulch, Dawson City, YT	metacarpal		
BS503	Y (all)		Bison	ADFG	RS-0001	Black R.. Yukon Flats, AK	metacarpal	2776±36	OxA-11631
BS504	Y (all)		Bison	CMN	CMN 49765	Eldorado Cr., Dawson City, YT	metacarpal		
BS505	Y (all)		Bison	CMN	CMN 25211	Flat Cr., Dawson City, YT	metacarpal	>50100	OxA-11957
BS507	Y (all)		Bison	PIN	MKh-01-461	Lena R. Delta, Bykovsky Pen., Siberia	bone		
BS509	N		Bison	AMNH	A-282-1835	Livengood, AK	metacarpal		
BS511	Y (all)		Bison	AMNH	A-691-4230	Goldhill, Fairbanks, AK	metapodial		
BS516	Y (all)		Bison	PIN	MKh-01-466	Lena R. Delta, Bykovsky Pen., Siberia	tibia		
BS517	Y (all)	C	Bison	ADFG	RS-0202	Birch Cr., Yukon Flats, AK	bone	2526±26	OxA-11989
BS531	Y	R	Bison	ChNRS	CRS-DY-22	Kolyma lowland, Duvanny Yar, Siberia	phalange		
BS532	Y	R	Bison	ChNRS	CRS-DY-25	Kolyma lowland, Duvanny Yar, Siberia	phalange		
BS533	Y (all)	C	Bison	ChNRS	CRS-IC-7	Kolyma lowland, Duvanny Yar, Siberia	femur		
BS539	Y (all)	R	Bison	ChNRS	CRS-DY-x2/40	Kolyma lowland, Duvanny Yar, Siberia	bone		
BS540	Y (>2/3)	R	Bison	ChNRS	CRS-PY-x1/5	Kolyma lowland, Plakhin Yar, Siberia	bone		
BS541	Y	R	Bison	ChNRS	CRS-DY-x3/27	Kolyma lowland, Duvanny Yar, Siberia	bone		
BS542	Y	R	Bison	ChNRS	CRS-DY-x4/542	Kolyma lowland, Duvanny Yar, Siberia	bone		
BS543	Y (>2/3)	R	Bison	ChNRS	CRS-DY-x5/37	Kolyma lowland, Duvanny Yar, Siberia	bone		
BS544	N		Bison	ChNRS	CRS-DY-x6	Kolyma lowland, Duvanny Yar, Siberia	bone		
BS559	N		Bison antiquus	MW	MW02	Vancouver Island, BC	skull	11750±110	
BS560	Y (all)		Bison	MW	#30, MW07	Hitching Post Ranch, Calgary, AB	tooth	2807±28	OxA-12123
BS561	Y (all)	C	Bison	ADFG	RS-0203	Porcupine R./Sucker R., AK	femur		
BS562	Y (all)		Bison	CMN	CMN 17304	Quartz Cr., Dawson City, YT	metacarpal		
BS563	Y (all)		Bison	MW	EaOq-3, MW04	Medicine Hat, AB	tibia		
BS564	Y (all)		Bison	PIN	3342-100c	Kolyma lowland, Siberia	pelvis	24570±90	OxA-11959
BS565	Y (all)		Bison	UAF	V-51-32	Chena R., Fairbanks, AK	metapodial		
BS566	N		Bison	MW	1.103/66, MW05	Folsom Site, NM	metapodial		
BS567	Y (all)		Bison	MW	#32, MW06	Hitching Post Ranch, Calgary, AB	tooth		
BS568	Y (all)		Bison	CMN	CMN 49621	Sulphur Cr., Dawson City, YT	metacarpal		

BS569	Y (all)	C, R	Bison antiquus	MW	EiPo-51, MW03	Hitching Post Ranch, Calgary, AB	metatarsal	3600±70	Beta-1627
BS570	Y (all)	C, R	Bison antiquus	MW	MW01	Gallelli Pit, Calgary, AB	metacarpal	11300±290	RL-757
BS571	Y (all)		Bison	ChLM	CRS-DY-34	Kolyma lowland, Duvanny Yar, Siberia	astragalus	32910±170	OxA-11958
BS572	Y (all)		Bison	CMN	CMN 33038	Old Crow, YT	skull		
BS574	Y (all)	C, R	Bison	YHR		Dawson City, YT	metacarpal	>52000	OxA-12028
BS575	Y (all)	C	Bison	YHR		Dawson City, YT	metacarpal		
BS578	N		Bison	PMA	Unit13 Levelx	Stampede Site, Cypress Hills, AB	bone		
BS579	N		Bison	PMA	P94.1.272	Cons. Pit 48, Edmonton, AB	bone		
BS582	Y (all)		Bison	PIN	IEM 202-0584	Novosibirsk Islands, Zimovye R., Siberia	tibia		
BS586	Y (all)	C	Bison	PIN	PIN 3657-139	Achchagyy-Allaikha, Siberia	bone	>62500	OxA-12125
BS590	Y (all)		Bison	PIN	PIN 3916-0	Mys Chukochiy, Rechnoye, Siberia	metatarsal		
BS592	Y (all)	C	Bison	ZMIPAE	887/3	Ekaterinburg, Urals, Russia	femur		
BS594	Y	C, R	Bison	PIN	PIN 3491-300	Kolyma lowland, Mal. Anyyu R., Siberia	ulna		
BS595	Y (all)		Bison	KU	KU 45337	Natural Trap Cave, WY	bone		
BS597	N		Bison	ZMIPAE	178/234	Ekaterinburg, Urals, Russia	astralagus		
BS598	N		Bison	KU	KU 127094	Kansas R., KS	bone		
BS602	Y (all)	C	Bison	KU	KU 127093	Kansas R., KS	mandible		
BS605	Y (all)	C, R(2)	Bison	KU	KU 51275	Natural Trap Cave, WY	femur	20380±90	OxA-12124
BS608	N		Bison	ZMIPAE	915/176	Ekaterinburg, Urals, Russia	metacarpal		
BS609	Y (all)		Bison	PIN	PIN 3913-61	Taimyrskoye Lake, Baikura-Neru Bay	skull		
BS610	N		Bison	ZMIPAE	178/41	Ekaterinburg, Urals, Russia	scapula		
BS643	N		Bison	PC	32748.939	Aufhausener Hohle, Germany	axis		
BS644	N	C	Bison		6516.3.9.72.1	Ludwigs hafey-Rheinhouhein, Germany	frontal		
BS646	N		Bison		DP1912	Los Reyes La Paz, Mexico			
BS647	N	C	Bison		5314	Oaxaca, Mexico	skull		
BS649	Y (all)	C	Bison	CMN	CMN 35780	Cripple Hill, Dawson City, Yukon			
BS650	N		Bison		SR-5980	Jake Bluff site, Oklahoma, USA			
BS651	N		Bison		SR-6060/ CHEM-7399	Cooper Site, Oklahoma, USA			
BS652	N		Bison		SR-6233/ CHEM-7383	Cooper Site, Oklahoma, USA			
BS653	Y		Bison		SR-6315/ CHEM-7605-7606	Cooper Site, Oklahoma, USA			
BS655	Y (all)		Bison	PIN	PIN 3100-153	Kolyma lowland, Chukochya Bol., Siberia	metacarpal		
BS656	Y (all)		Bison	PIN	PIN 3915-103	Indigirka lowland, Umnas Lake, Siberia	metacarpal		
BS658	Y (all)		Bison	PIN	PIN 3020-092	Kolyma lowland, Syapyakine R., Siberia	metacarpal		
BS659	Y (all)		Bison	PIN	BL-O 736/PIN 202-0736	Novosibirsk Islands, Zimovye R., Siberia	radius		
BS660	Y (all)		Bison	ZMIPAE	994/252	Ekaterinburg, Urals, Russia	metapodial		
BS662	Y (all)		Bison	PIN	PIN 3658-131	Kolyma lowland, Alyoshkina Zaimka, Siberia	metacarpal		
BS663	Y (all)		Bison	PIN	PIN 3100-422	Kolyma lowland, Chukochya Bol., Siberia	metacarpal		

BS664	Y (all)	Bison	PIN	PIN 3020-297	Kolyma lowland, Bochanut Lake, Siberia	metacarpal
BS665	Y (all)	Bison	PIN	PIN 3915-164	Kolyma lowland, Bochanut Lake, Siberia	metacarpal
BS667	Y (all)	Bison	PIN	PIN 3915-240	Indigirka lowland, Tastakh Lake, Siberia	metacarpal
BS670	Y (all)	Bison	PIN	PIN 162-018	Kolyma lowland, Alazeya, Siberia	metatarsal
BS672	Y (all)	Bison	PIN	PIN 3751-016	Yana region, Omoloy River, Siberia	metatarsal
BS673	Y (>2/3)	Bison	PIN	PIN 161-59	Indigirka lowland, Kerememesit R., Siberia	calcaneous
BS674	Y (all)	Bison	ZMIPAE	816/166	Ekaterinburg, Urals, Russia	phalange
BS677	Y (all)	Bison	PIN	PIN 3100-507	Kolyma lowland, Chukochya Bol., Siberia	metacarpal
BS678	Y (all)	Bison	PIN	BL-O 851/PIN 202-0851	Novosibirsk Islands, Zimovye R., Siberia	mandibula
BS681	Y (all)	Bison	PIN	PIN 153-111	Indigirka lowland, Vorontsovskiy Yar, Siberia	metacarpal
BS682	Y (all)	Bison	PIN	PIN 3100-552	Kolyma lowland, Chukochya Bol., Siberia	metacarpal
BS687	Y	Bison	PIN	PIN 3657-172	Indigirka lowland, Achchagyy-Allaikha, Siberia	metatarsal
BS689	Y (all)	Bison	PIN	PIN 3341-0868	Kolyma lowland, Chukochya Bol., Siberia	metacarpal
BS690	Y (all)	Bison	PIN	PIN 3915-168	Indigirka lowland, Tastakh Lake, Siberia	metacarpal
BS691	Y (all)	Bison	PIN	BL-O 598/PIN 202-0598	Novosibirsk Islands, Zimovye R., Siberia	metacarpal
BS692	Y (all)	Bison	PIN	BL-O 744/PIN 202-0744	Novosibirsk Islands, Zimovye R., Siberia	tibia
BS693	Y (all)	Bison	PIN	BL-O 559/PIN 202-0559	Novosibirsk Islands, Zimovye R., Siberia	calcaneous
BS694	Y (all)	Bison	PIN	PIN 3342-109	Kolyma lowland, Khetachan, Siberia	ulna
BS696	Y (all)	Bison	PIN	M9-4	Lena R. Delta, Bykovsky Pen., Siberia	metatarsal
BS697	Y (all)	Bison	PIN	PIN 3752-044	Kolyma lowland, Duvanny Yar, Siberia	metacarpal
BS698	N	Bison	PIN	PIN 164-065	Kolyma lowland, Mal. Anyuy R., Siberia	metacarpal
BS699	N	Bison	PIN	2494-810/51-p	NE Kazakhstan (Pavlodar region), Russia	bone
BS700	Y (all)	Bison	PIN	PIN 165-132	Indigirka lowland, Khomus-Yuryakh Bol. R., Siberia	metacarpal
BS701	Y	Bison	PIN	PIN 835-30	Kolyma lowland, Chukochya Bol., Siberia	antebrachium
BS702	Y	Bison	PIN	PIN 3491-347	Kolyma lowland, Mal. Anyuy R., Siberia	metacarpal
BS703	Y (all)	Bison	PIN	PIN 3915-268	Indigirka lowland, Volchya R., Siberia	metacarpal
BS704	N	Bison	ZMIPAE	888/1681	Ekaterinburg, Urals, Russia	Scapula
BS705	Y (all)	Bison	PIN	PIN 161-134	Indigirka lowland, Kerememesit R., Siberia	metacarpal

BS706	Y (all)		Bison	PIN	PIN 3915-165	Indigirka lowland, Tastakh Lake, Siberia	metacarpal		
BS707	Y (all)		Bison	PIN	PIN 3021-024	Kolyma lowland, Yakutskoye Lake, Siberia	metacarpal		
BS708	Y (all)	C, R	Bison	ZMIPAE	888/47	Ekaterinburg, Urals, Russia	femur		
BS712	Y (all)		Bison	PIN	PIN 3913-062	Taimyr Peninsula, Taimyrskoye Lake, Siberia	metacarpal		
BS713	Y (>2/3)	C, R	Bison	ZMIPAE	915/166	Ekaterinburg, Urals, Russia	metatarsal		
BS719	Y (all)	C, R	Bison	YHR	YG 127.1	Christie Mine, Dawson City, Yukon	metacarpal		
BS726	N		Bison latifrons	IMNH	48001/181	American Falls, ID	metatarsal		
BS728	N		Bison latifrons	IMNH	815/17393	American Falls, ID	metacarpal		
BS729	N		Bison latifrons	IMNH	65003/28910	American Falls, ID	calcaneous		
BS730	N		Bison latifrons	IMNH	50001/15215	American Falls, ID	ulna		
BS731	N		Bison latifrons	IMNH	65001/32165	American Falls, ID	metatarsal		
BS732	N		Bison latifrons	IMNH	65001/16653	American Falls, ID	rib		
BS733	N		Bison latifrons	IMNH	48002/32118	American Falls, ID	cranium		
BS734	N		Bison latifrons	IMNH	35015/17306	American Falls, ID	metacarpal		
BS735	N		Bison latifrons	IMNH	71005/26115	American Falls, ID	humerus		
BS736	N		Bison latifrons	IMNH	71003/26667	American Falls, ID	astragalus		
BS737	N		Bison latifrons	IMNH	48001/16870	American Falls, ID	metatarsal		
BS738	N		Bison latifrons	IMNH	783/18253	American Falls, ID	metacarpal		
BS739	N		Bison latifrons	IMNH	35015/16187	American Falls, ID	sacrum		
BS741	N		Bison latifrons	IMNH	72001/23386	American Falls, ID	phalange		
BS742	N		Bison latifrons	IMNH	50001/334	American Falls, ID	phalange		
BS743	N		Bison latifrons	IMNH	75002/27	American Falls, ID	metacarpal		
BS744	N		Bison latifrons	IMNH	35015/5460	American Falls, ID	sacrum		
BS745	N		Bison latifrons	IMNH	35015/17116	American Falls, ID	metatarsal		
BS746	N		Bison latifrons	IMNH	71004/17407	American Falls, ID	radius		
BS747	N		Bison latifrons	IMNH	GRCA 55974	Stanton's Cave, Flagstaff, AZ	hoof		
BS775	N		Bison	ZMIPAE	915/164	Ekaterinburg, Urals, Russia	metacarpal		
BS776	N		Bison	ZMIPAE	915/7	Ekaterinburg, Urals, Russia	calcaneous		
BS777	N		Bison	ZMIPAE	178/164	Ekaterinburg, Urals, Russia	metatarsal		
BS778	N		Bison	ZMIPAE	178/42	Ekaterinburg, Urals, Russia	ulna		
BS779	N		Bison	ZMIPAE	577/47	Ekaterinburg, Urals, Russia	mandible		
BS780	N		Bison	ZMIPAE	915/139	Ekaterinburg, Urals, Russia	mandible		
IB070	Y (all)		Bison	UAF	V-54-21	Lost Chicken Cr., Chicken, AK	metacarpal		
IB071	Y (>2/3)		Bison	UAF	V-54-25	Lost Chicken Cr., Chicken, AK	metacarpal		
IB072	Y (all)	C	Bison	UAF	V-54-117	Lost Chicken Cr., Chicken, AK	cranium		
IB073	Y (all)		Bison	UAF	V-54-134	Lost Chicken Cr., Chicken, AK	metapodial		
IB178	Y (>2/3)		Bison	UAF	V-54-295	Lost Chicken Cr., Chicken, AK	metapodial		
IB179	Y (all)		Bison	UAF	V-54-320	Lost Chicken Cr., Chicken, AK	metapodial	12465±75	OxA-111
IB180	Y (all)	C	Bison	UAF	V-54-16	Lost Chicken Cr., Chicken, AK	metapodial		

Table S2: Primers Used. The following primers were used to amplify the 685-bp fragment of the mitochondrial control region. Numbers refer to the position of the 3' base in the cow mitochondrion (Genbank) NC10057.

Forward primers	
BISCR-16348F	CTACAGTCTCACCGTCAACCC
BISCR-16355F	ACCCCCAAAGCTGAAGTTCT
BISCR-16420F	CCATAAATGCAAAGAGCCTCAC
BISCR-16506F	ACTAGCTAACGTCACTCACCCC
BISCR-16512F	CCACTAGCTAACGTCACTCACCCC
BISCR-16633F	GCCCCATGCATATAAGCAAG
BISCR-16697F	CGTACATAGCACATTATGTC
BISCR-16710F	GCACATTATGTCAAATCTACCCTTGACAAC
BISCR-16762F	CACGAGCTTAACTACCATGC
BISCR-16765F	GAGCTTAAYTACCATGCCG
BISCR-16876F	CAGACATCTGGTTCTTTCTTCAG
BISCR-16975F	TGGGGGTCGCTATTTAATGA
Reverse Primers:	
BISCR-16499R	GGGGTGAGTGACGTTAGCTAGT
BISCR-16652R	TAAGTACTTGCTTATATGCATGGGGC
BISCR-16532R	GGGGTGAGTGACGTTAGCTAGTG
BISCR-16612R	CTTGCTTATATGCATGGGGC
BISCR-16642R	GCATGGGGCATATAATCTAATGTAC
BISCR-16652R	TAAGTACTTGCTTATATGCATGGGGC
BISCR-16721R	GATTTGACATAATGTGCTATG
BISCR-16729R	CAAGGGTAGATTTGACATAATGTG
BISCR-16810R	GCCTAGCGGGTTGCTGGTTTCACGC
BISCR-16871R	GATGTCTGATAAAGTTCATTAAATAGCGACCCC
BISCR-16886R	CCAGATGTCTGATAAAGTTCA
BISCR-16990R	GATGAGATGGCCCTGAAGAA
BISCR-53R	CCAAATGTATGACAGCACAG
BISCR-80R	CAAGCATCCCCCAAAATAAA
BISCR-94R	GGCCATAGCTGAGTCCAAGC

Table S3: Summary of the results of the Bayesian analyses (a) excluding Western Beringia (b) excluding both Western Beringia and central North America and (c) including all samples with finite radiocarbon dates. In (a) two MCMC chains were run for 30 million iterations, assuming the two-epoch model as described for the complete analysis. For (b) and (c) five MCMC chains were run as described above. The age of the root of the tree, the initial growth rate prior to the peak population size, the date that the population reached the peak, and the size of this peak as a multiple of the size of the modern population, are presented as mean values (bold) plus the lower and upper 95% highest posterior density (HPD) of values.

	(a) Excluding W. Beringia			(b) Eastern Beringia Only			(c) Complete Analysis		
	lower	**mean**	upper	lower	**mean**	upper	lower	**mean**	upper
Age of root (years BP)	104,000	**130,000**	157,000	95,750	**132,000**	177,000	111,000	**136,000**	164,000
Initial growth rate	4.21E-05	**6.57E-05**	9.02E-05	3.87E-05	**6.73E-05**	9.87E-05	4.48E-05	**6.78E-05**	9.23E-05
Time of peak (years BP)	31,000	**36,000**	41,400	25800	**31,300**	36900	32,500	**37,400**	43,500
Spike factor	43	**155**	305	62	**1374**	3876	71	**237**	454

Table S4: Summary of the demographic results of the Bayesian analyses of the modern clade (1a of Fig. S2) assuming (a) constant population size, (b) exponential growth and (c) a two-epoch demographic model. In each analysis, two MCMC chains were run for 20 million iterations as described for the main analysis. The first 1.5 million iterations were discarded from each chain and the remainder were combined. Values for the transition/transversion ratio, proportion of invariant sites, and the gamma distribution were fixed to the mean estimated value from the full analysis. Results are presented as mean values and lower and upper 95% HPD values.

	Constant Size			**Exponential growth**			**Two-epoch**		
	lower	**mean**	upper	lower	**mean**	upper	lower	**mean**	upper
a. Age estimates (years B.P.)									
Root Height	17,200	**28,200**	41,000	12,800	**17,400**	23,200	11,700	**14,900**	18,600
Transition time (population peak)	N/A	**N/A**	N/A	N/A	**N/A**	N/A	63	**910**	2,300
b. Model parameters									
Mean ln(posterior)		**-1822**			**-1818.4**			**-1794**	
Pre-transition/ exponential growth rate	N/A	**N/A**	N/A	1.07E-04	**2.54E-04**	4.13E-04	1.96E-04	**4.88E-04**	8.11E-04
Peak population size (relative to current size)	N/A	**N/A**	N/A	N/A	**N/A**	N/A	1	**790**	4000
Current effective population size	12,300	**22,600**	34,500	22.2	**102,000**	218,000	11,700	**14,900**	18,600

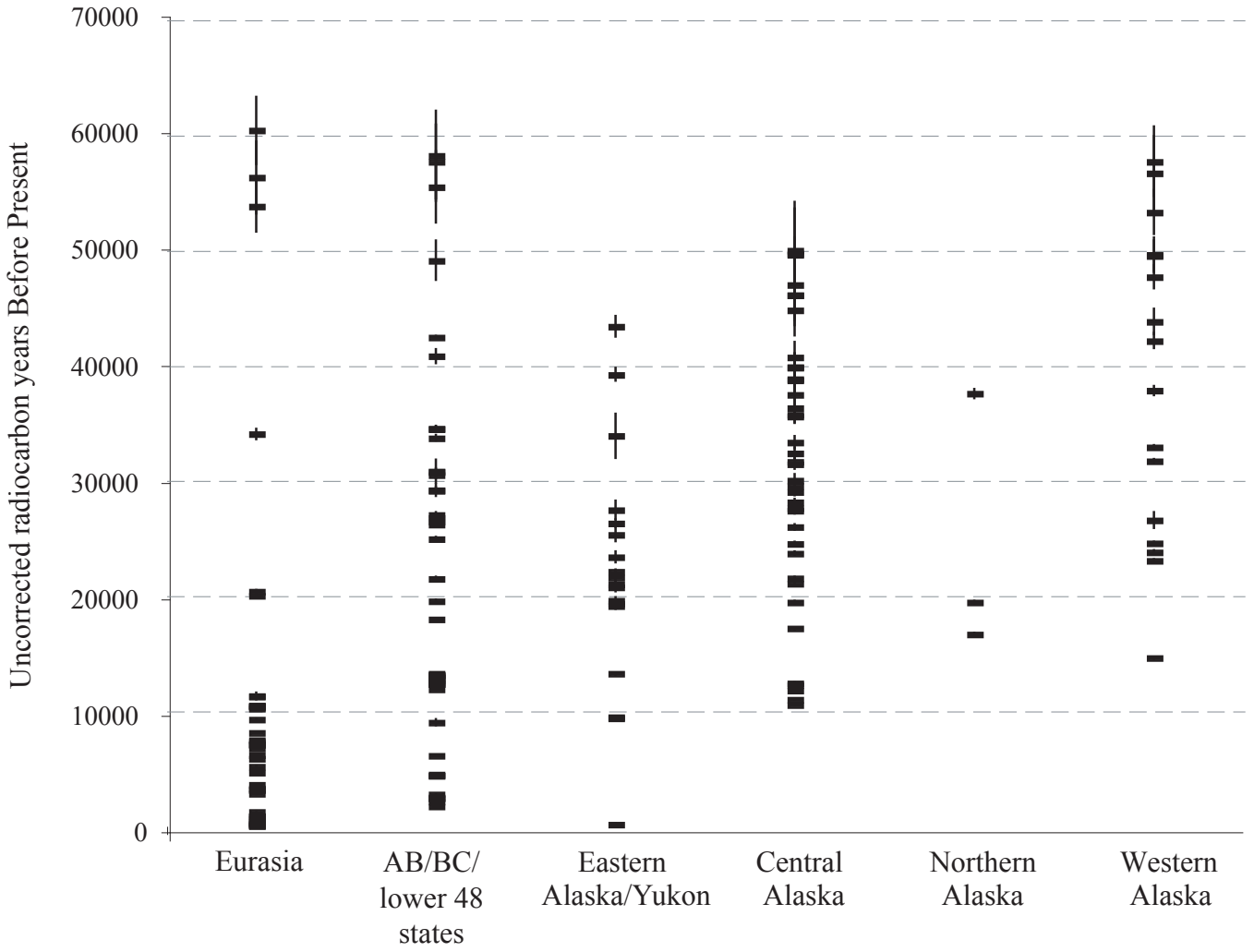

Fig S1. Distribution of the 169 fossil bison associated with finite radiocarbon dates that were used in the full Bayesian phylogenetic analysis. Bars show 95% confidence intervals of the radiocarbon date. Radiocarbon accession numbers associated with specific specimens are given in Table S1.

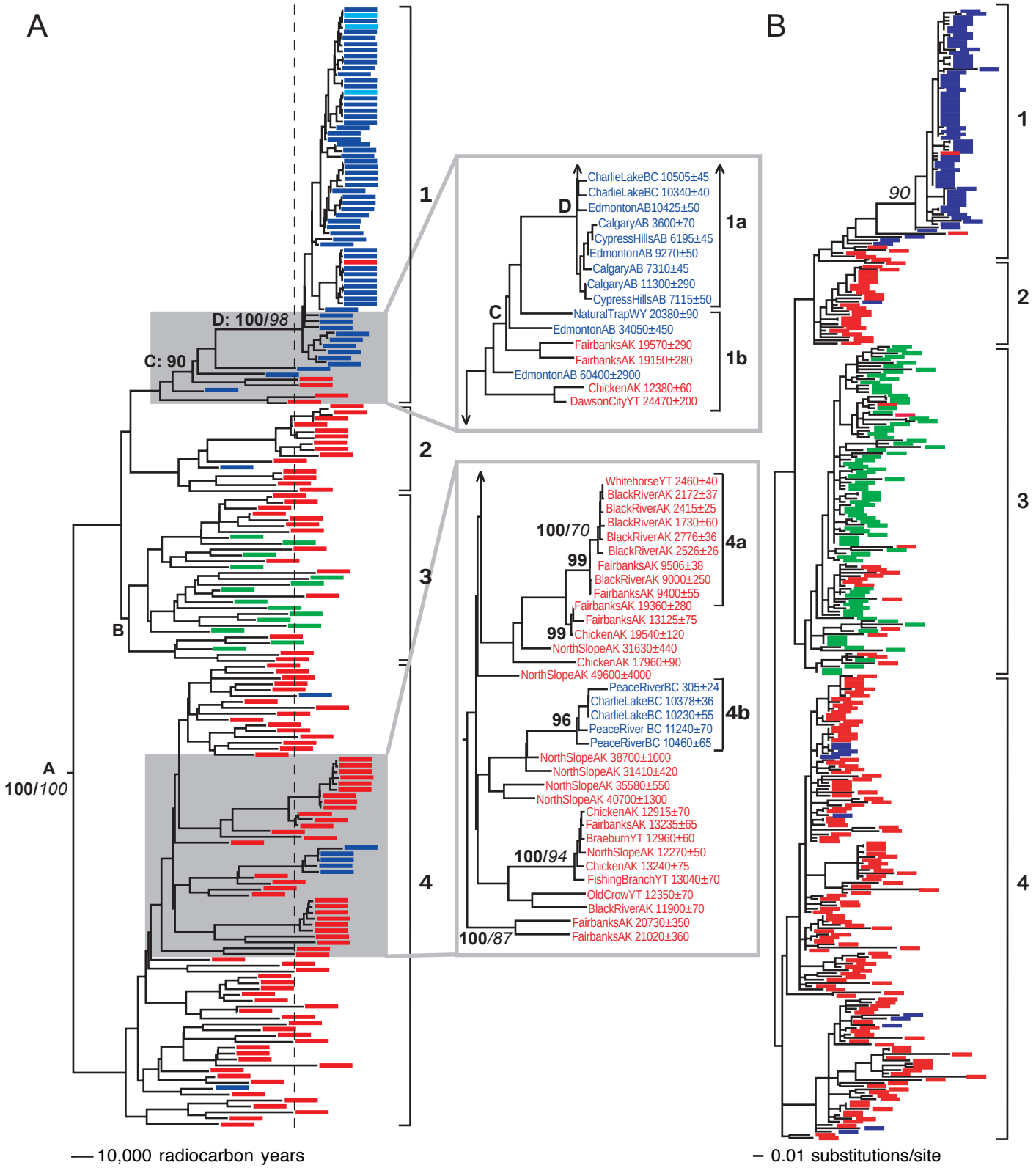

Figure S2: Results of phylogenetic analyses. (A) MAP tree from the Bayesian analysis of 169 ancient and 22 modern bison with Bayesian posterior probabilities ≥90% (bold) and Neighbor-joining (NJ) bootstrap resampling support values ≥70% (italics); and (B) NJ tree showing relationships among 352 bison for which ≥2/3 of the 665-bp control region fragment was sequenced, with the NJ bootstrap result for clade 1a. Bayesian analyses were performed using BEAST(S4), while the NJ tree and bootstrap results were generated with PAUP*(S8) assuming a HKY+G+I model with parameter values set to the mean values obtained in the two-epoch Bayesian analysis (Table 1, main text). For simplicity, the trees have been divided into 4 major clades and several subclades. Colours indicate geographical origins of the samples: green – Asia and W. Beringia, red – E. Beringia, blue – North America south of Beringia. Branch tips to the right of the dashed vertical line (A) are associated with radiocarbon dates <20 ka BP.

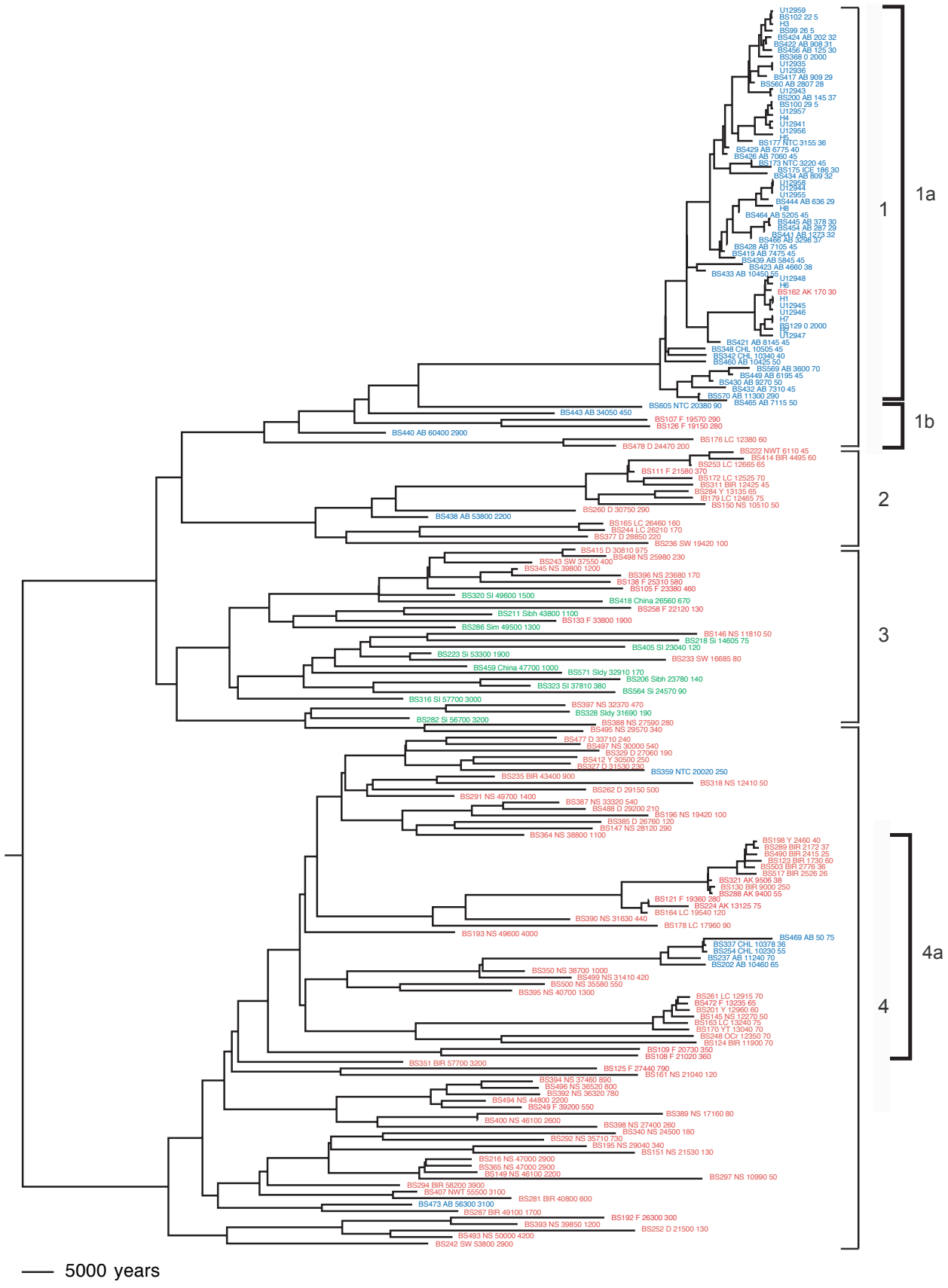

Figure S3: Detailed version of Fig S2a. Geographic locations and radiocarbon dates are given at the nodes. Colors are as follows: red - Eastern Beringia, green – Western Beringia, blue – North America south of Beringia. Clade identification as in Fig. S2.

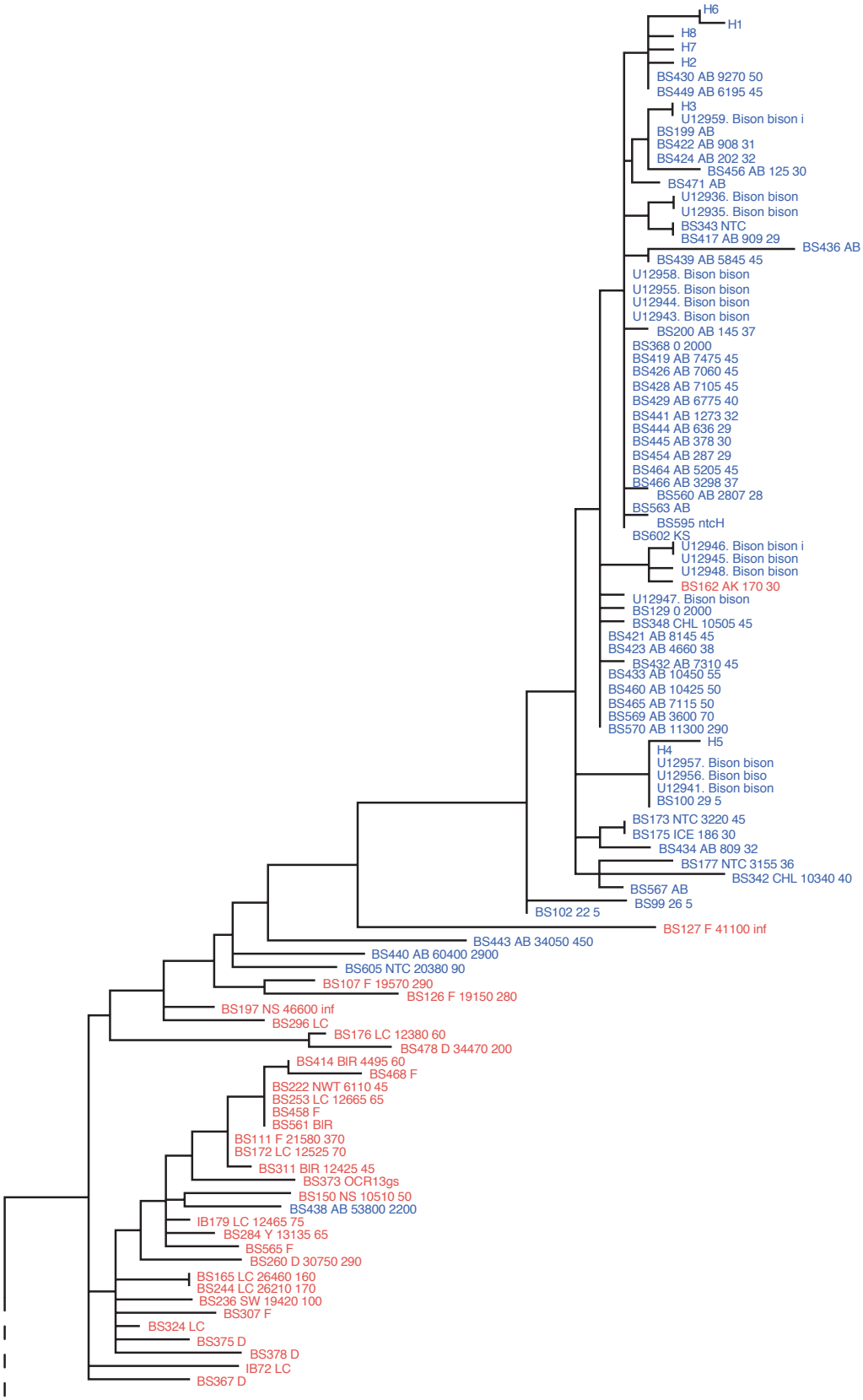

Figure S4a: Part 1 of 3 of a detailed version of Fig S2b. Geographic locations and radiocarbon dates (when available) are listed at the tips. Colors are as in Fig. S3.

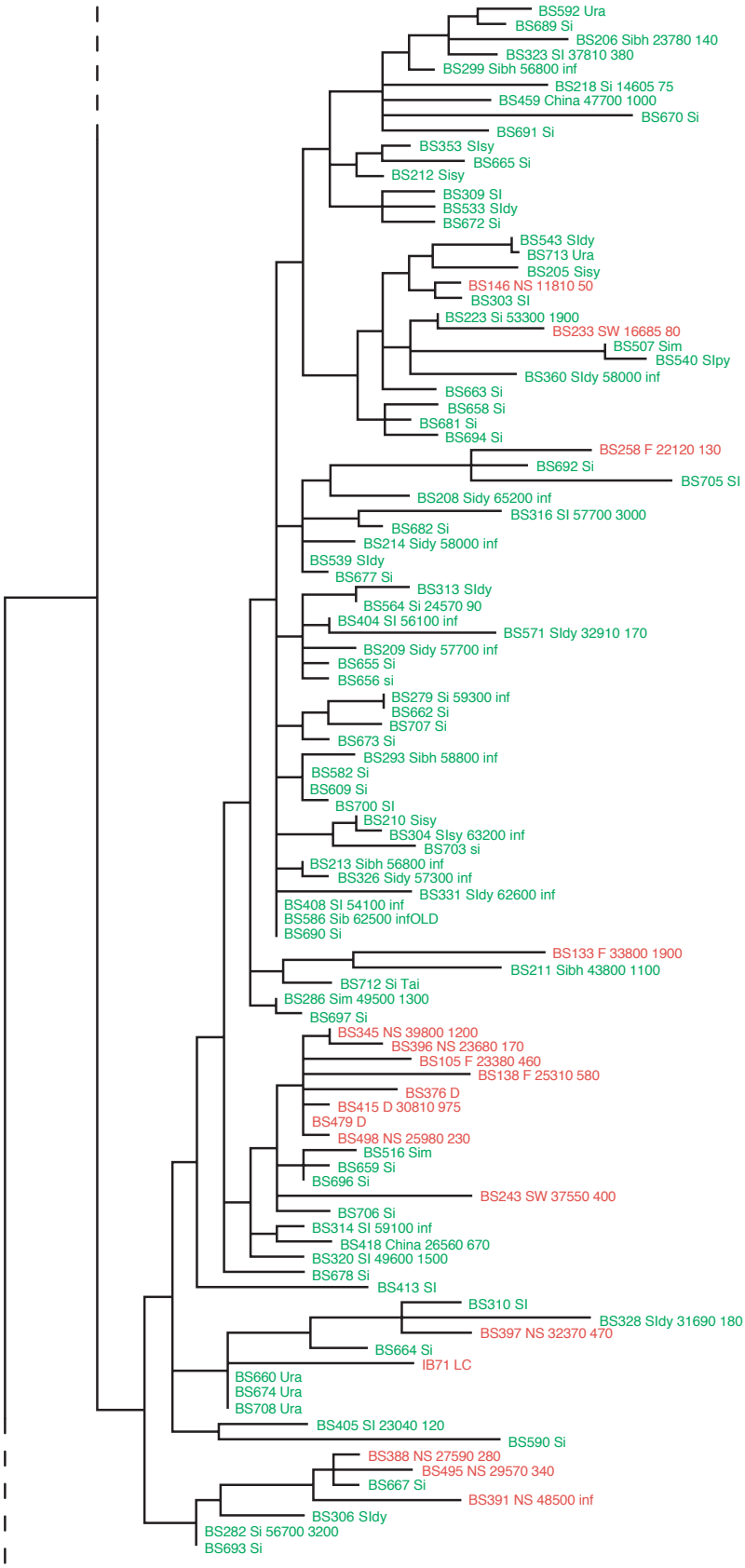

Figure S4b: Part 2 of 3 of a detailed version of Fig S2b. Geographic locations and radiocarbon dates (when available) are listed at the tips. Colors are as in Fig. S3.

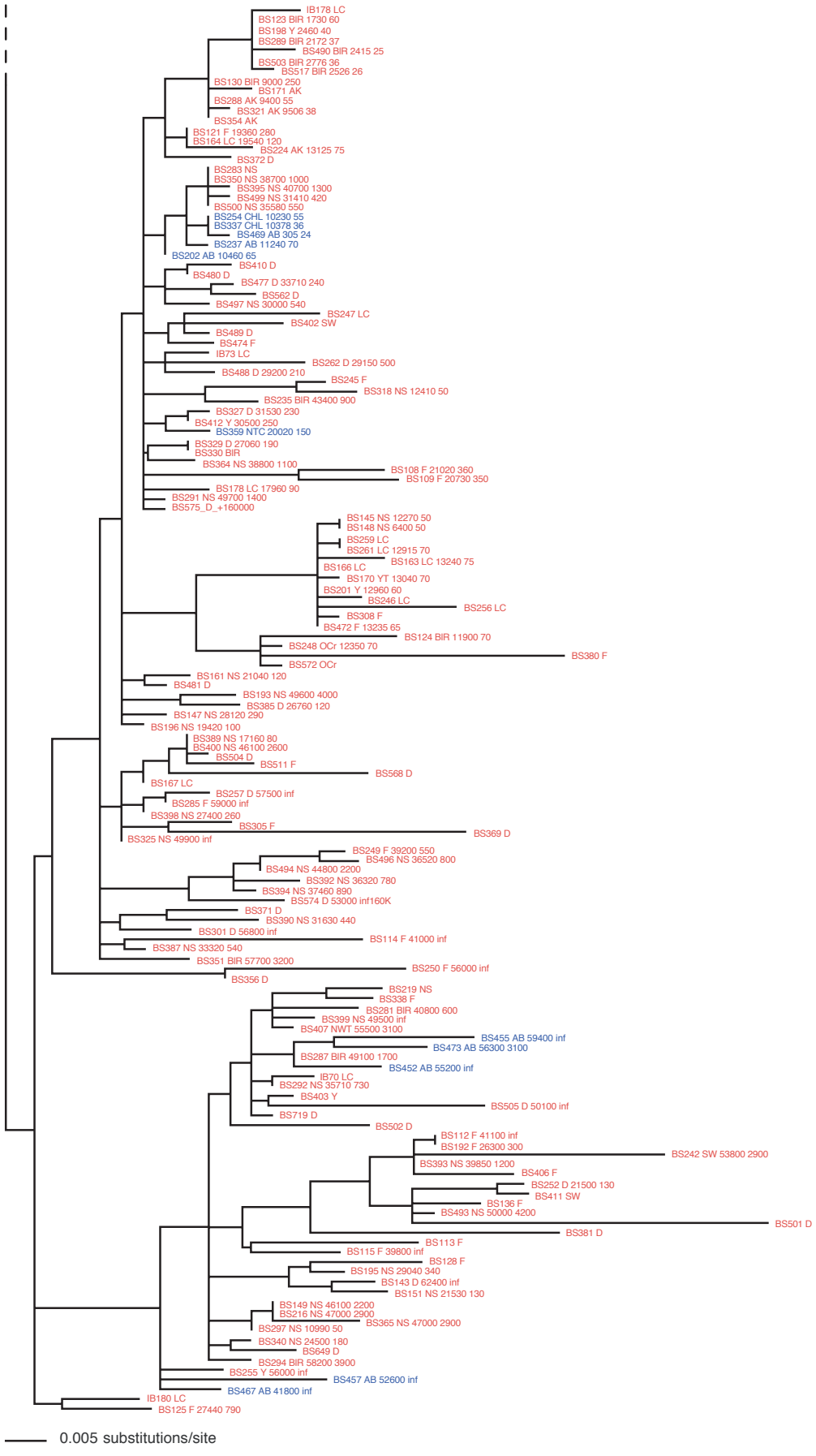

Figure S4c: Part 3 of 3 of a detailed version of Fig S2b. Geographic locations and radiocarbon dates (when available) are listed at the tips. Colours are as in Fig. S3.

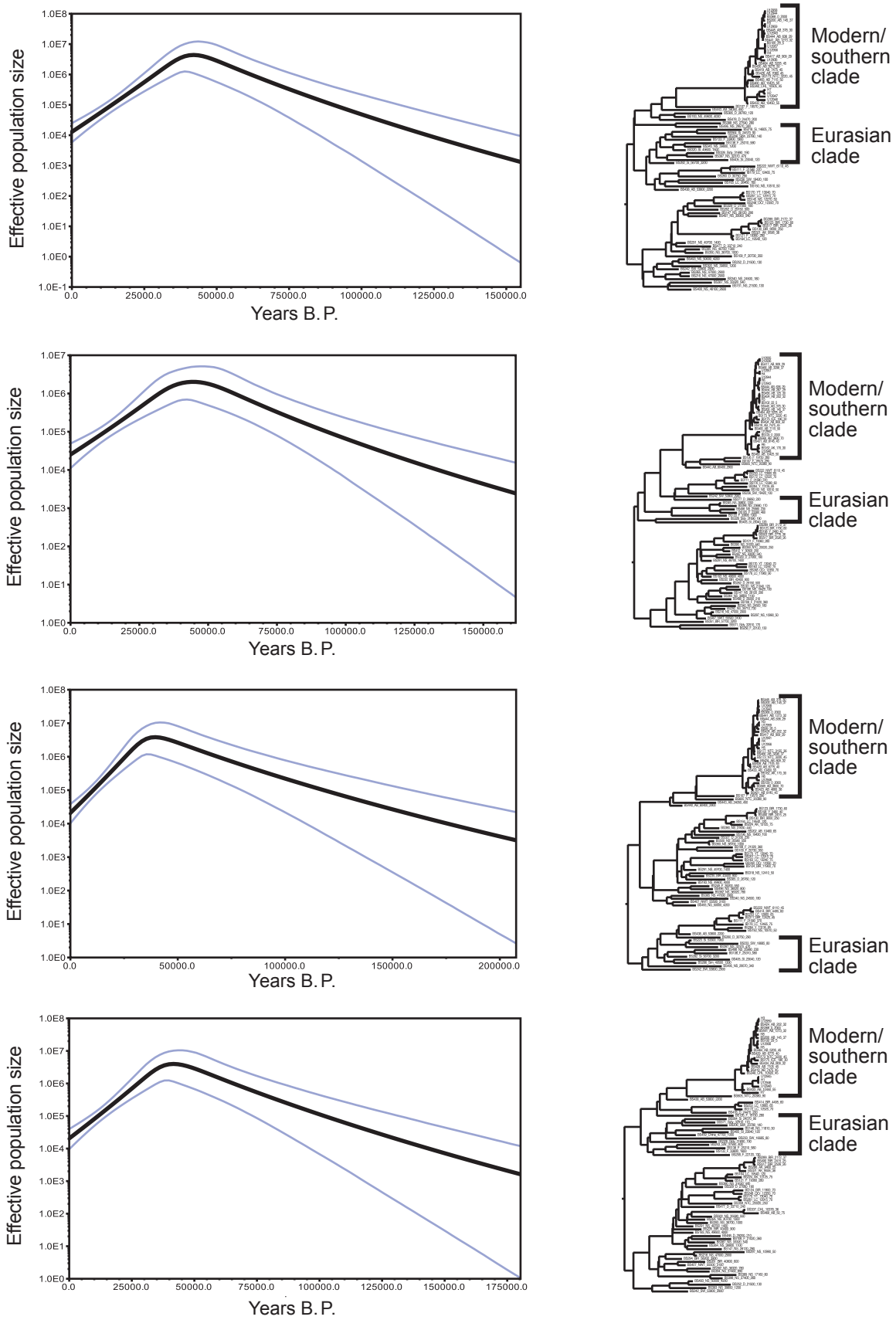

Figure S5: Results of the two-epoch Bayesian analyses of 4 randomly chosen subsets of the complete dataset. Each analysis was performed as in the main analysis, except only one MCMC chain of 30 million iterations was run for each subset, with the first 3 million iterations discarded as burn-in. Although the power of the analyses was reduced by the limited data, the results of the demographic analyses were consistent with those of the full analysis, and each of the major clades is represented in the MAP trees.

References:

S1. E. L. C. Verkaar, I. J. Nijman, M. Beeke, E. Hanekamp, J. A. Lenstra, *Mol. Biol. Evol.* 21, 1165 (2004).

S2. J. N. McDonald, *North American Bison: Their Classification and Evolution* (Univ. of California Press, Berkeley, 1981).

S3. A. Cooper, H. N. Poinar, *Science* 289, 1139 (2000).

S4. A. J. Drummond, A. Rambaut, BEAST v. 1.x available from http://evolve.zoo.ox.ac.uk/beast (2004).

S5. A. J. Drummond, G. K. Nicholls, A. G. Rodrigo, W. Solomon, *Genetics* 161, 1307 (2002).

S6. W. K. Hastings, *Biometrica* 57, 97 (1970).

S7. D. J. Spiegelhalter, N. G. Best, B. R. Carlin, A. van der Linde, *J. Roy. Stat. Soc. Ser. B - Stat. Method.* 64, 583 (2002).

S8. D. L. Swofford. {PAUP}* Phylogenetic analysis using parsimony (*and other methods) (Sinaur, Sunderland, MA, 1999).

S9. O. G. Pybus, A. Rambaut, *Bioinformatics* 18, 1404 (2002).

S10. K. Strimmer, O. G. Pybus, *Mol. Biol. Evol.* 18, 2298 (2001).

S11. B. O. K. Reeves, in *Hunters of the Recent Past* L. B. Davis, B. O. K. Reeves, Eds. (Unwin Hyman, London, 1990) pp. 168-194.

S12. G. A. Wilson, C. Strobeck, *Genome* 42, 483 (1999).

S13. R. O. Polziehn, R. Beech, J. Sheraton, C. Strobeck, *Can. J. Zool.-Rev.* 74, 738 (1996).